TRANSFER LEARNING APPROCH FOR DETECTING COVID-19 USING CHEST X-RAY IMAGES

Muthunayakage Nimesha Asintha Muthunayake

209359G

M.Sc. in Computer Science

Department of Computer Science and Engineering
Faculty of Engineering

University of Moratuwa
Sri Lanka

July 2022

TRANSFER LEARNING APPROCH FOR DETECTING COVID-19 USING CHEST X-RAY IMAGES

Muthunayakage Nimesha Asintha Muthunayake
209359G

Thesis/Dissertation submitted in partial fulfillment of the requirements for the degree of
Master of Science in Computer Science

Department of Computer Science and Engineering
Faculty of Engineering

University of Moratuwa
Sri Lanka

July 2022

DECLARATION

I declare that this is my own work and this thesis does not incorporate without acknowledgement any material previously submitted for a Degree or Diploma in any other University or institute of higher learning and to the best of my knowledge and belief it does not contain any material previously published or written by another person except where the acknowledgement is made in the text. Also, I hereby grant to University of Moratuwa the non-exclusive right to reproduce and distribute my thesis, in whole or in part in print, electronic or other medium. I retain the right to use this content in whole or part in future works.

Signature: Date:

The above candidate has carried out research for the Master's thesis under my supervision. I confirm that the declaration made above by the student is true and correct.

Name of the supervisor:

Signature of the supervisor: Date:

ACKNOWLEDGEMENTS

I wish to express my sincere gratitude to my supervisor, Dr. Charith Chitraranjan, for his guidance and invaluable assistance in providing me with useful knowledge materials, advice, and supervision throughout this research work. His expertise and encouraging guidance enabled me to complete my work successfully.

I am indebted to my parents for their love and untired support throughout my life.

ABSTRACT

Due to the (COVOD-19 coronavirus, the entire world is undergoing a pandemic. Coronavirus 2 produces severe acute respiratory illness. This virus is discovered in December 2019 in China, Wuhan. As we are experiencing, the affected patients are expanding at a rapid rate. The World Health Organization (WHO) has recommended that testing be done as much as possible to recognize those who are affected and those who are carriers of this disease. However, the main issue here is the scarcity of COVID-19 testing kits and trained people to perform the testing in a pandemic situation. However, a lot of research was seeking workaround solutions for detecting the COVID-19. As a result of these projects, a few papers were polished for detecting the COVID-19 based on chest X-ray scan images. However, most of the research has used vanilla CNN, which makes the test more reliable and convenient. But we have some practical issues in the application of traditional CNN. Basically, CNN is a supervised learning method, and it takes more time for the learning process. And in general, CNN works well for larger datasets. However, the chest X-ray images are limited in practice, we propose combining transfer learning and ensemble learning techniques to achieve excellent accuracy while spending the least amount of time possible on the entire learning process. This study mainly focuses on the CNN based pre-trained models such as **DenseNet201, EfficientNetB7 and VGG16** for increasing the accuracy level of the model, which makes the test reliable and more trustworthy.

TABLE OF CONTENTS

LIST OF FIGURES

LIST OF TABLES

LIST OF ABBREVIATIONS

Abbreviation	Description
RNA	Ribonucleic Acid
PCR	Polymerase Chain Reaction
CT	Computerized Tomography
RT-PCR	Reverse Transcription Polymerase Chain Reaction
ARDS	Acute Respiratory Distress Syndrome
CO2	Carbon Dioxide
O2	Oxygen
VGG16	Visual Geometry Group
ANN	Artificial Neural Network
ReLU	Rectified Linear Unit
FC	Fully Connected Layer
RESNET	Residential Energy Services Network
ANOVA	Analysis of Variance
ML	Machine Learning
NLP	Natural Language Processing
CAM	Class Activation Map

1. CHAPTER 1: INTRODUCTION

1.1 Background

In December 2019, the first instance of the novel coronavirus illness (COVID-19) was reported in Wuhan, China. Following that, it spread over the world as a COVID-19 outbreak. This pandemic is disgraceful because the outbreak has a flow of several waves. Due to the RNA mutation process, the second wave is deadlier than the first wave. The number of confirmed cases has risen to 1000 in just a few months, with over 5000 first-degree suspect cases. By the end of September 2020, this deadly disease had spread across the entire world, crossing many oceans. At the time this paper was being written, the total reported cases were more than 255,458,171 and more than 5,135,192 confirmed deaths worldwide [1]. In general, the SARS-CoV-2 virus has two types of attack levels: mild and severe. In both scenarios, the lungs and airways swell and become inflamed. At this level, doctors advise keeping track of the patients in terms of their blood oxygen level in order to detect and treat any abnormalities [2].

The coronavirus naturally attacks the human lungs at the initial stage and leads to pneumonia in severe situations [3] [4] [5] [6] [7] [8] [9] [10]. Consequently, it reduces the oxygen level in the blood due to the negative effects on the affected lungs. As we already know, at the time of writing, there is no medicine or cure for this disease. The only recommendation is to prevent getting affected by the virus. Therefore, tracing the patients and testing the suspected people is the only solution. When it comes to testing, PCR (Polymerase Chain Reaction) is widely used in medicine in order to detect and confirm cases. However, doing enough PCR testing as the number of cases grew in the midst of the bloodiest outbreak was a major difficulty. On the other hand, PCR takes a long time to process and produce a result; during this period, the patient can easily touch other people and spread the disease without realizing what is going on. As we already know, many developing countries, like Sri Lanka, have a limited number of PCR machines to perform the tests. Therefore, naturally, people have to wait in a long queue to get their PCR results in order to confirm whether the suspected person is COIVID-19 positive or negative. On the other hand, there should be specifically trained people to perform PCR testing. In general, in a pandemic situation like COVID-19, a shortage of trained people is normal in nature. Therefore, it is a risk to totally depend on the entire test on PCR or on one particular test. In addition, it is time-consuming and costly. As a result, a workaround solution is needed to detect infected people as early as possible during a pandemic by speeding up the quarantine or isolation process, which is particularly effective at stopping the spread of this deadly disease over the entire country. Deep neural network and latest machine learning technologies are currently being utilized to detect the COVID-19 virus.

However, the outcomes and outputs of these methodologies are insufficient for them to be used as medically acknowledged diagnosis systems.

As a workaround, this project provides a machine learning method to recognize COVID-19 positive patients using their chest X-ray images. The internal image of human lungs can be utilized to successfully detect COVID-19 patients in general. As we already know, most government and private hospitals have at least one X-ray machine since it is a primary requirement of the medical diagnosis process. But the manual method of using X-ray scanning also causes some additional issues and concerns. It requires expert medical practitioners and extra time to analyze the X-ray scanning images. Therefore, a supervised deep learning approach can be used for classifying COVID-19 infected people from their chest X-ray images [11].

1.2 How does the COVID-19 virus affect a person's lungs?

COVID-19 infected patients need to reveal whether they are infected by COVID-19 so they can obtain relevant self-isolation or treatments as soon as possible. As we already discussed, diagnosing COVID-19 requires a **PCR** or **Rapid Antigen Test** using throat and nasal samples. For RT-PCR tests, there should be specific tools, and in addition, it takes at least 24 hours to prepare the report. COVID-19 is a respiratory disease. Normally, medical practitioners may use a lung x-ray to diagnose people who have virus infected symptoms, until the PCR result is ready.

In general, COVID1-9 can result in severe pulmonary effects like pneumonia, sepsis, and ARDS (Acute Respiratory Distress Syndrome). All these complications cause harm to the human lungs directly. Based on the analysis, a serious pro-inflammatory condition called severe COVID-19 can cause a number of serious consequences, syndromes, and diseases. normally in pneumonia lungs become filled in inflamed and fluid. It leads to critical breathing difficulties. In some cases, these breathing issues can become severe enough to require ventilator or oxygen treatments at the hospital.

COVID-19 pneumonia has a high-level tendency to infect both human lungs. Small air sacs in the lungs fill with fluid, and it limits the lung’s ability to take in oxygen. This may lead to shortness of breath and a severe cough. There is little lung damage in some patients who survive from COVID-19 pneumonia. Some people have catastrophic damage or failures in their lungs even after the disease has passed.

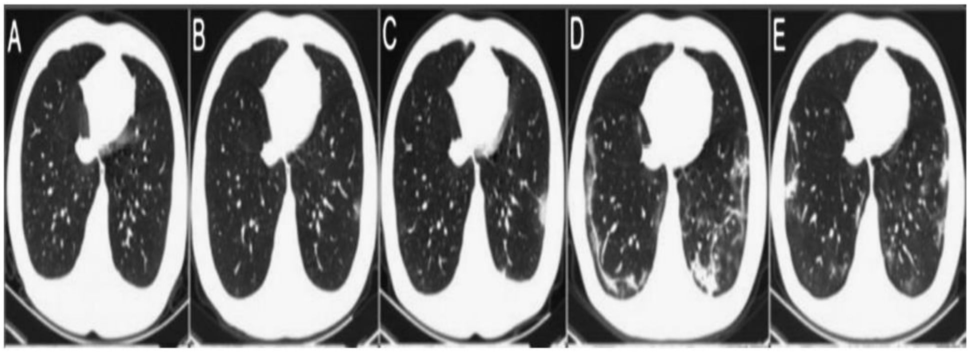

Figure 1.1: COVID -19 Pneumonia Progression General Steps

Figure 1.1 shows the basic process inside the lungs of a COVID-19 patient. It shows the gradual changes in the opacities in the human lungs. Initially, there were no significant changes in the X-ray image. But as time increases, it shows some bilateral changes inside the lungs. And the rest of the X-ray images show the progression of COVID-19 pneumonia with linear ground glass opacities in the subpleural areas of the human lung [12]. In this chapter, we propose that X-ray images can be used to identify infected people. However, in general, chest scanning images have low sensitivity and high attentiveness to modeling the lung opacity changing process [13].

1.2.1 Acute Respiratory Distress Syndrome (ARDS)

Acute respiratory distress syndrome is a life-threatening and severe lung injury that allows fluid to leak inside the lungs. As a result, breathing becomes difficult and oxygen cannot get into the body. Most patients who get acute respiratory distress syndrome are already at the hospital for illness or trauma. People with ARDS may need ventilator support since they can't breathe on their own and can't get enough oxygen into their blood without it. Patients who survive ARDS and COVID-19 may have long-lasting pulmonary scarring. In general, ARDS can be lethal [14].

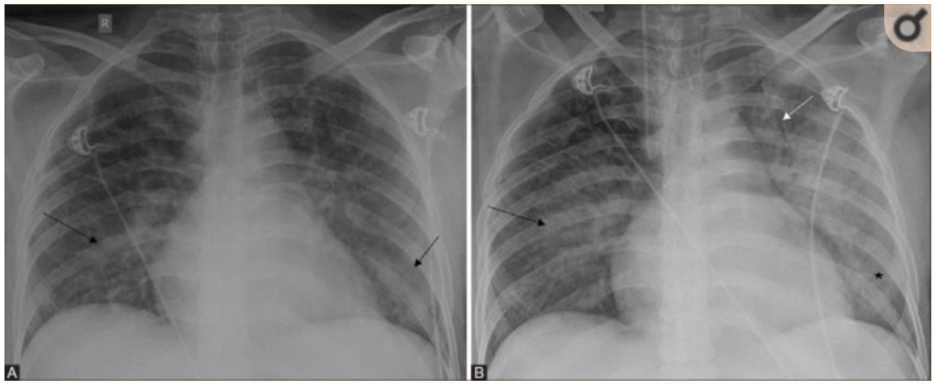

Figure 1.2 : (ARDS) is a Condition in Which the Body's Respiratory System, the Images Shows the Damages Done by ARDS to the Human Lungs [15]

Figure 1.3 depicts the interstitial architecture of the human lungs, which may result in airspace opacification due to flooding of protein-rich fluid. Figure 1.2 shows how the characteristics of a simple film of the exudative phase of the human lung resemble those of cardiogenic pulmonary edema. However, the absence of root apex circulatory redistribution and cardiomegaly in the former, as well as normal vascular pedicle peribronchovascular (the connective tissue sheath that encloses the bronchi, pulmonary arteries, and lymphatic vessels), improved cuffing and internal cuffing and internal pleural effusion in the latter [16].

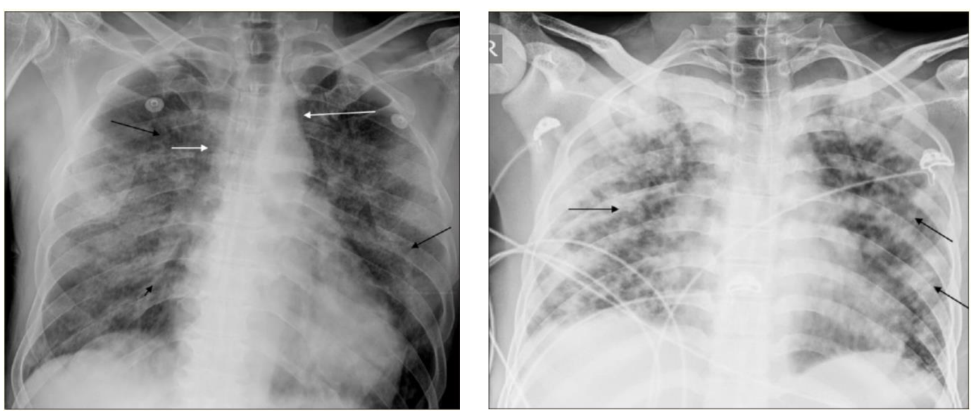

Figure 1.3: Bilateral Reticular Opacities, Normal Human Vascular Pedicle Width

1.2.2 Sepsis

Sepsis is another feasible complication of the COVID-19 infection. Sepsis generally occurs when an infection spreads and enters the human bloodstream. This can lead to serious tissue damage everywhere. As we already know, the heart and lungs work together with other organs. It breaks down the coordination of each organ in the body. Sepsis, to put it another way, is the body's overreaction to an infection. It's a medical emergency of some sort. Changes in human mental status, systolic blood pressure, and higher respiratory rate are the main symptoms of sepsis. In addition, septic shock drops the human blood pressure, which gives bad results in normal daily activities and energy production. Even if sepsis survives, patients can still experience catastrophic damage to the human lungs and other related organs. Figure 1.4 shows microorganisms that are likely to cause sepsis and general pneumonia of pulmonary origin, together with their primary x-ray resource symptoms [17].

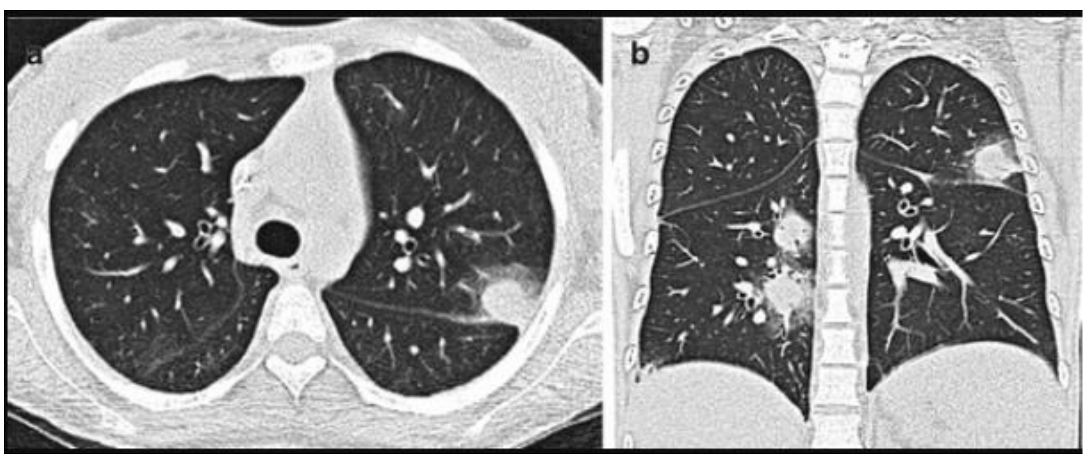

Figure 1.4: (a, b) A 20-year-old Woman with Invasive Pulmonary Aspergillosis had Soft Tissue Nodules Covered by the Ground Glass Opacity of the Lung on an Axial and Coronal HRCT.1.2.3 Viral Pneumonia

In general, pneumonia is a type of lung illness brought on by bacteria, fungi, and viruses. Viral pneumonia is caused by viral bodies and most frequently the symptoms can be seen in elderly people and young children. The crucial problem here is that viral pneumonia leads to inflammation in the human lungs. It causes abnormal circulation of oxygen (O2) and carbon dioxide (CO2) in the alveoli. Viruses which are known to cause viral pneumonia include the parainfluenza virus, herpes virus, respiratory syncytial virus, human metapneumovirus, adenovirus, enteroviruses, rhinovirus, hantavirus, varicella-zoster virus, measles virus (rubeola), influenza A virus, and coronavirus. If pneumonia is identified, a medical practitioner may ask for additional tests, including a chest CT scan, chest x-ray, blood culture, complete blood count, swab test, sputum culture, blood gas test, and open lung biopsy [18].

A CT scan or X-ray of the human chest is usually done to imagine the severity and location of the inflammation in the lungs. Using the lungs' x-ray images, certain characteristics that can be used to dissimilarly detect viral pneumonia include bilateral infiltrates, patchy distribution of interstitial infiltrates, and interstitial infiltrates. Furthermore, thin section thoracic X-ray is specifically significant for detecting specific attributes of viral-pneumonia.

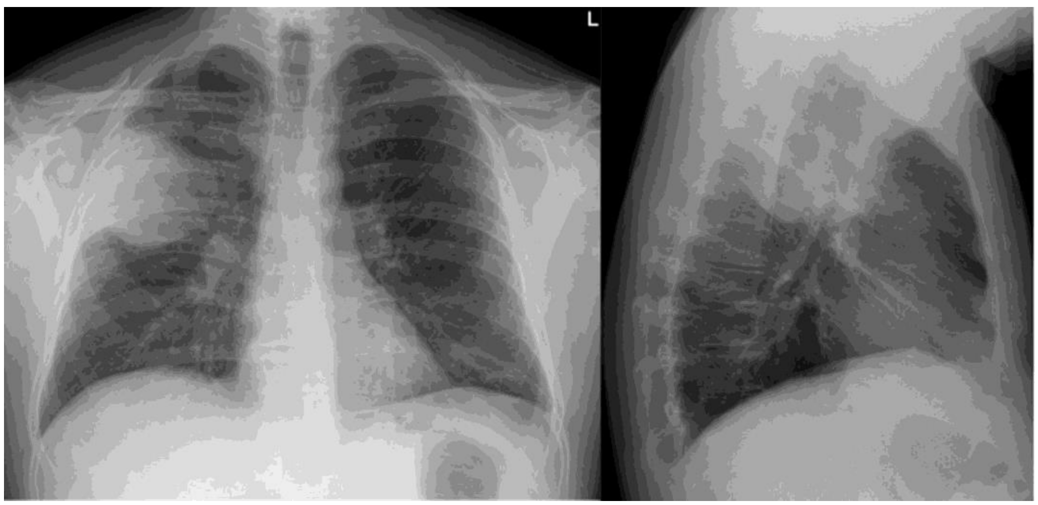

Figure 1.5: Chest X-rays Taken on Admission in an Affected Human Lungs with Round Pneumonia.

Figure 1.5: shows a human admission lung’s x-ray image for an old man (50 year), and it shows round pneumonia symptoms in the lungs with a specific pattern in opacities. The contrast between a pneumonic and a normal chest X-ray is seen in Figure 1.6. A pneumonic condition can be distinguished from a healthy condition by pneumonic X-ray infiltrates, or white patches (red arrows are used as an example) [19].

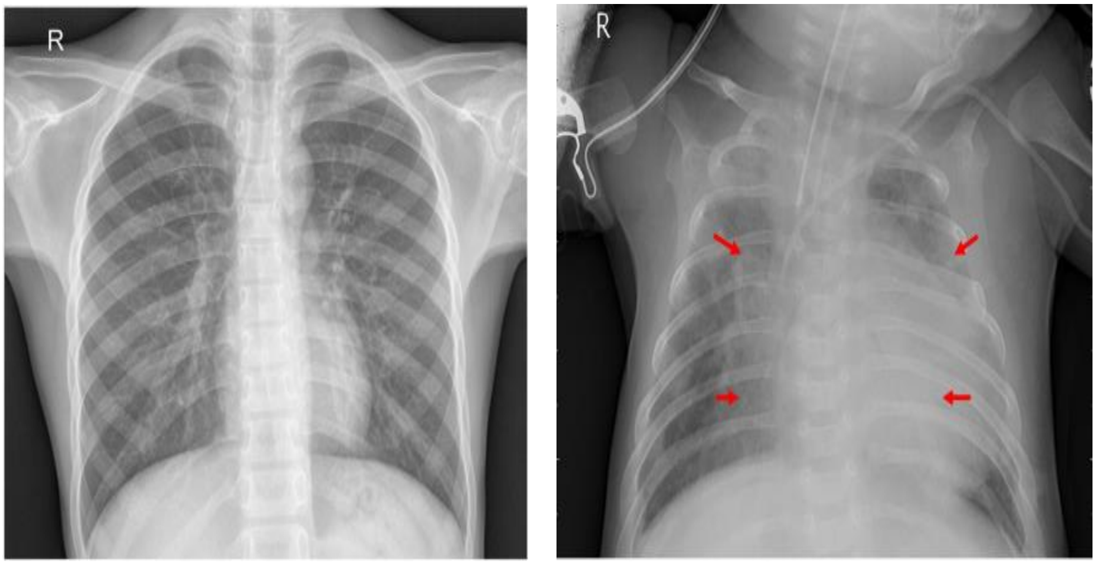

(a) (b)

Figure 1.6: Images of Normal and Pneumonia Affected Human Lungs Taken Via X-ray. A Healthy Lung and a Pneumonic Lung are the Two Types of Lungs. White Infiltrates are Indicated by the Red Arrows in (b) [20].

1.3 Research Problem

The major goal of this research is to find answers to the following research questions:

As explained in the above section, PCR is the main testing methodology being used by many countries to detect COVID-19 patients in their society for managing the quarantine and isolation process. However, due to the lack of PCR machines and PCR operators who can manage the PCR detection procedure, many patients have to be on the waiting list to take their PCR results during the peak time of the pandemic situation. On the other hand, PCR procedures are time consuming and costly, so there is a proper research gap to have an efficient and fully automated alternative detection mechanism.

A few faults in earlier studies were discovered, including the use of imbalanced datasets and a minimal number of X-ray images to train the deep learning model, both of which significantly impacted the performance of these deep neural models and their ability in making predictions. In addition to that, many previous studies used two classes of images to train the deep learning model. These two class-based models can only perform well when provided with COVID-19 negative and positive images. The main limitation behind this is that these models cannot properly classify non-COVID pneumonia and COVID-19 pneumonia because, most of the time, both cases have similar symptoms and opacities in the lung X-ray images.

1.4 Motivation

In addition to laboratory tests, chest X-ray images may be effective in identifying COVID-19 in people with a high clinical suspicion of infection. The X-ray images represent the important bones, organs, tissues, and vessels. And it allows doctors to analyze the internal body structures and see their size, shape, texture, and density. X-ray images provide much more relevant and accurate details of the patients. This information can be used to determine whether there is a COVID-19 virus attack or not. On the other hand, X-ray machines and related operators are widely available in the hospital domain. A person cannot imagine a hospital without X-ray machines since they are a fundamental requirement in medical diagnosis procedures. Therefore, it is motivated to continue this project using X-Ray images.

As we already know, convolutional neural networks are highly effective in terms of image classification. In general, reusing a pre-trained deep learning model on a new problem is called "transfer learning." It can train a deep neural network using a small amount of data. Since we have limited X-Ray scanning images as a dataset, we use the transfer learning model in order to get high throughput. Ensemble machine learning techniques always give better prediction results and achieve better performance than any single model. In general, ensemble, learning is a meta technique for machine learning that gives high accuracy and better performance by combining the predictions from a few predictive models. Therefore, it has motivated us to perform an ensemble learning approach to achieve high predictive performance and accuracy in terms of the COVID-19 detection classification problem.

1.5 Research Objectives

The main objectives of this proposed study are

The major goal of this study is to determine the classification accuracy and the limitations of this COVID-19 detection method using X-ray images. The rest of the objectives of this project are as follows.

- Designing and developing a deep learning model to detect corvid-19 pneumonia versus general pneumonia.

- Implementing a deep neural network model using a pre-trained model such as DenseNet, EfficientB7, and VGG16 in order to save resources and improve the efficiency of the training process.

- Use an ensemble learning approach to combine the results of DenseNet, EfficientB7, and VGG16 together to improve the performance.

1.6 Thesis Structure

The following is how the rest of the article is structured: The Literature Review is discussed in Chapter 2, which focuses on previous research on text data classification in banking. The research approach will be detailed in Chapter 3, and the research will be concluded in References.

2. CHAPTER 2: LITERATURE REVIEW

2.1 Overview

Since COVID-19 has been widely disseminated throughout the world, many types of research have been published in the fields of artificial intelligence and medical analysis in order to automate the general diagnostic procedure. We will emphasize a few topics in this chapter: COVID-19, pneumonia, and normal patients are detected using binary and multi-class classification. This chapter focuses on cutting-edge machine learning methods for categorizing X-ray images and identifying COVID-19 positive people in society during the COVID-19 outbreak. CT scanning X-ray image datasets are widely used by many recent researchers in discussing the advantages and limitations of the X-ray image approach [21,22]. Also, top-performing machine learning models have been summarized for detecting the coronavirus using CT scanning images [23]. To stress the CT infection area and opacities in the human lungs, an automated quantification and segmentation approach with machine learning and image segmentation has been introduced. [24]. Tianjin Medical University has developed a deep learning algorithm to extract X-ray image attributes [25]. Huazhong University of Science and Technology (HUST) [26] used a three-dimensional artificial neural network (ANN) based on a weekly supervised machine learning model to detect lung images to diagnose COVID-19 pneumonia using three-dimensional (3D) X rays.

2.2 Convolutional Neural Network

In general, X-ray pictures are used as input data, and they are preprocessed before being fed to the deep learning model. There are two types of classes: COIVID -19 patients and normal patients. Splitting the dataset, re-sizing images into proper sizes, and data augmentation are widely used methods in the convolutional mural network approach. As we already know, fine-tuning and filtering always increase the accuracy of the prediction model. Therefore, in the above block diagram, they have used these general techniques as usual for better accuracy. Once the data is in the model, analyzing the model accuracy, model loss, and confusion matrix helps to show how model loss functions change over time with model accuracy. In this model diagram, the entire data flow is illustrated in a simpler way [27].

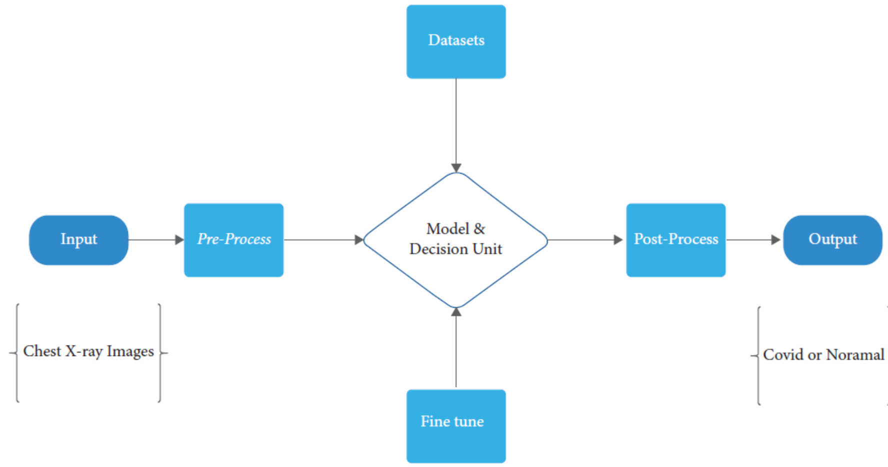

Figure 2.1: High-level Block Diagram of the General Flow of the Learning Process [12]

Similar research was done using the Convolutional Neural Network. However, 224 * 224 shaped images were used , and there were three channels. The 32-filter size was used with padding in the first two layers of the introduced network architecture. They employed a kernel width of 3 and the ReLU activation function, resulting in the front max-pooling layer, which contains a stride of 2 and a pool size of 2. And here, two dense layers were used, with the first layer being ReLU and the second layer being SoftMax. This is the overall system architecture most of the researchers used for implementing the convolutional neural network efferently [28] [29].

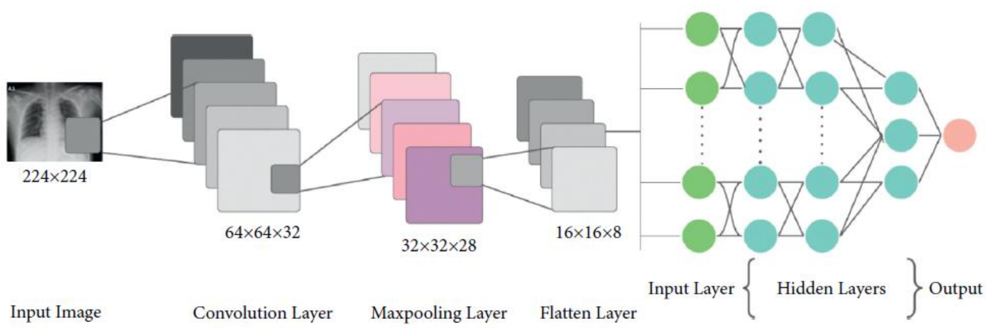

Figure 2.2: Overall System Architecture for Convolutional Neural Network

The convolutional layer, as we are all aware, is the base of a convolutional neural network. This layer is used to specify the deep learning model's design characteristics. This layer's incoming image is processed through a filter. The output of the same filter generates the function map. A convolution process handles the inputs and modification of a set of weights. Typically, a 2D collection of weights multiplied by the whole input data array makes up the filters in this layer. A conventional neural network (CNN) is used by Li et al. to detect COVID-19 infected patients from chest X-ray images. Here they used the above common method in order to get a high COVID-19 prediction accuracy [30]. In general, the CNN model can be used for classification feature extraction. Many of the studies have used filter-based feature extraction in convolutional neural network models, which can increase the predictive performance. As described in some papers, CNN is best suited for classifying images with hilly complex identities. Using the above common convolutional neural network architecture, a considerable number of weighted parameters can be turned down [31]. In addition, one of the best CNN-based learning models is implemented by the Cancer Hospital of Tianjin Medical University for extracting the COVID-19 image features and analyzing the COID-19 positive cases, providing well-explained theories and concepts of accurate and timely diagnosis [32].

2.3 Transfer Learning

Nowadays, transfer learning is one of the most widely used approaches in deep learning techniques. It always provides the flexibility of training a smaller dataset with less time and higher accuracy than the vanilla method. There are pre-trained machine learning models on extremely large datasets. These pre-trained models can be used to transform the model into different subject areas. As we described in a previous chapter, most medical data, such as X-ray pictures, is available in smaller datasets. With transfer learning techniques, it is possible to train a deep learning model using a small dataset without overfitting the model [33]. In general, the final layer is removed from the pre-trained network; after that, it will be replaced by a new layer that can be fitted with the new class. The typical pooling in prior experiments was 4 * 4 fully linked networks with a dropout of 0.5. The last network layer has two classes related to COVID-19 positive and negetive X-Ray images with a loss function of binary cross-entropy [34].

In previous studies, one experimental architecture was proposed in order to get high prediction performance in the deep learning model. According to this architecture, Pre-trained ResNet152, VGG19, DenseNet201, InceptionResNetV2, and Exception models are used to extract the X-ray lung image features. The last of the three FC layers in most network topologies is utilized for image categorization. The FC layer is replaced with a global average pooling layer beneath the deep learning neural network. It helps to effectively turn down the number of training parameters. As shown in Figure 2.3: this neural network architecture uses the five CNN structures in order to extract future maps. Each model is interconnected with the flattening layer and the global average pooling layer. Despite the fact that the FC layer has 3 layers, they set the drop-off to 0.5. While the third level is linked to a dense layer with one hidden unit, the first two levels are connected to a thick layer with 512 hidden units [35].

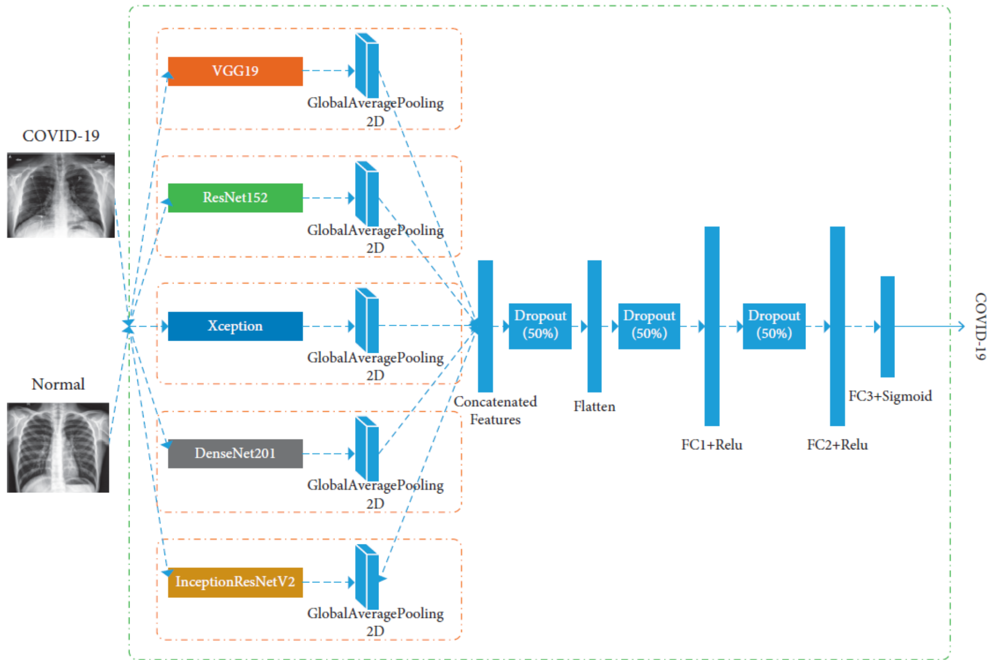

Figure 2.3: Common Cascade Network Model Diagram for Transfer Learning Process [20]

2.3.1 VGG16

In general, VGG16 is a very popular CNN architecture that was introduced in 2014. VGG16 is still one of the best classification models specially designed for image classification problems. Figure 2.4 depicts the high-level layout of the VGG16 classification model architecture, which has 16 network layers with convolutional layers with 3 × 3 filters and max-pooling layers stacked between them. In this study, the ReLU activation function is employed, as well as three fully connected layers that include the majority of the parameters in the classification model. The exact probabilities for each x-ray image classification are generated using the SoftMax function. With a prediction accuracy of 98 %, precision of 98 %, recall (also known as sensitivity), of 99 %, and an F1-score of 98.8 % for the calcification model, it outperforms the validation image data set [36].

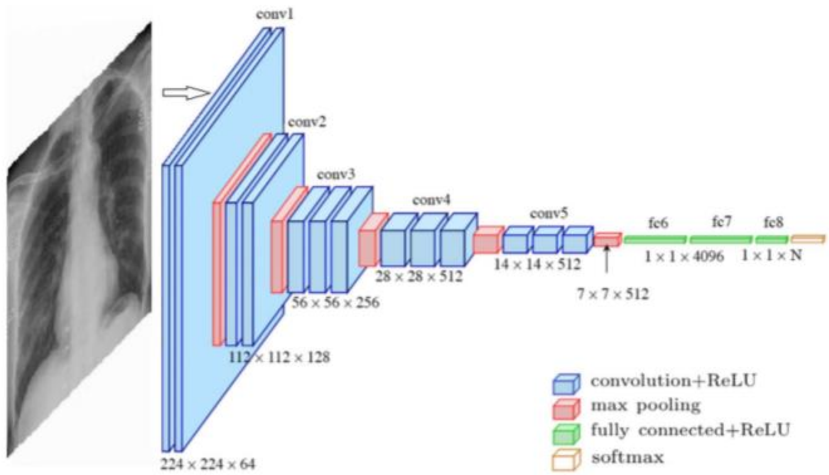

Figure 2.4: Pre-Trained VGG16 Classification Model High-level Architecture

In addition, VGG16 is used for one of the previous studies by modifying the last layer using a similar architecture to classify the X-ray images. Here the accuracy is 95.9% [37]. The VGG16 classification model suggested by Catak and Sahinbas is comparable, although it has a poor prediction impact. In this scenario, the model accuracy rate, F1-measure, recall, and precision are all at 80% [38].

2.3.2 DenseNet201

In many of the studies related to DenseNet201, which is associated with convolutional neural networks, has been densely used. DenseNet201 is designed with 201 default network layers. Every layer receives all of the previous layers' aggregate knowledge. As a result, it will create a densely compact network. In general, the vanishing gradient is a huge challenge in deep neural networks. Therefore, DenseNet201 is specially designed to address this problem by skipping connections similar to ResNet [39]. As we already know, in ResNet, features are combined using summation while features are concatenated with each other in DenseNet. The patterns of the connectivity are introduced by DenseNet to reduce the required parameters while training in the model. In general, it is highly effective in terms of the memory usage of the classification model. The total accuracy of the DenseNet201 model for COVID-19 detection is 92% [40]. An interesting study was done by Mundher Mohammed Taresh and Ningbo Zhu. They used DenseNet201 with image augmentation for the learning model. Here they achieved an accuracy of 97.94% for DenseNet201 [41]. In addition, there is a study done by Jenish Maharja and a team using six different transfer learning models, including DenseNet201. In this proposed method, they received 97% accuracy for DenseNet201 [42]. Another study done by Hemdan et al, reported that DenseNet201 accuracy is 90% with the similar chest X-ray image dataset [43].

2.3.3 EfficientNetB7

Based on the AutoML MNAS framework, a new network model was constructed. As expected, this paradigm enhances forecast accuracy and model efficiency. This model was scaled up to generate a model family called EfficientNets. In general, EfficientNetsB7 is one of the sub-models in this family, and it does not contain any pre-trained weights. As shown in Figure 2.5, similar to the other architectures, EfficientNets has 7 blocks. EfficientNetB0 is the base model, and the entire family of EfficientNets from B1 to B7 provides state-of-the-art ImageNet efficiency [44]. EfficientNetB7 is used to create a state-of-the-art x-ray image categorization model. Here in this study, the most interesting thing was that they used all the EfficientNetsB0 to EfficientNetsB7 models belonging to the family, including EfficientNetsB7. Here the accuracy is reported as follows in Table 2.1 [45].

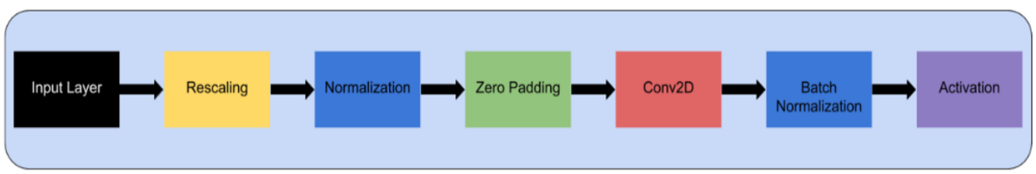

Figure 2.5: The Common Bocks Representation EfficientNets Architecture

Model	Accuracy (%)	Precision (%)	Recall (%)	F1-Score (%)
EfficientNetB0	95	95	95	95
EfficientNetB1	96	96	96	96
EfficientNetB2	96	96	95	95
EfficientNetB3	96	96	95	95
EfficientNetB4	94	94	93	94
EfficientNetB5	97	96	96	96
EfficientNetB6	95	95	95	95
EfficientNetB7	**95**	**95**	**95**	**95**

Table 2.3:Accuracy Matrix for EfficientNet Family [30]

2.4 Ensemble Learning

A common technique for combining the outputs of various machine learning models to produce a final output prediction for the test data sample is ensemble learning. It is achieved by taking the selective knowledge from all the base models, and producing a more accurate prediction result than the individual calcification models. Weighted average probability, majority voting, and average probability are some of the most commonly utilized ensemble approaches in studies. The average probability-based ensemble learning methods provide equal priority to each combining base learner. There are three primary types of ensemble learning approaches. Bagging, stacking, and boosting are the three methods.

Any machine learning problem's final aim is to find a perfect model that will offer us the best forecast as promised. Instead of developing a single model and hoping this ML model is the best (most accurate) clarifier we can introduce, the ensemble approach takes a myriad of models into account. The ensemble method will produce one final model with high accuracy in terms of prediction. Ensemble learning is the most cutting-edge deep learning approach for detecting pneumonia [46]. For the majority of earlier research, segmented chest x-ray images were utilized to train a mask region-based Convolutional Neural Network (CNN) for the identification of pneumonia. For picture thresholding, they employed a consolidated model that combined ResNet-101 and ResNet-50 [47]. Some studies emphasized the use of a deep transfer learning ensemble of ResNet-18, DenseNet-121, and GoogLeNet to deal with the shortage of available data for a specific problem. However, it employs a weighted average ensemble method in similar circumstances. The results were superior to those obtained using state-of-the-art methods, and their methodology outperformed commonly used generic ensemble approaches. The strength of the model is shown by analyzing the dataset using ANOVA and McNemar's tests. [48].

2.5 Data Set

Chest X-ray information is frequently used in medical research and is crucial to the COVID-19 detection method. Most medical practitioners can more easily detect the imaging modal characteristics of COVID-19 instances (changes) with the use of diagnostic chest imaging, such as interstitial changes and numerous small patchy shadows in the preliminary phase that are immediately outside the lungs. COVID-19 causes a variety of infiltration shadows and ground glass in both lungs. Lung condensation and pleural effusion are presumably uncommon in serious instances. It can be a useful guide for appropriately assessing progress and its current status.

The human lung X-ray COVID-19 dataset contains the subfolders NORMAL, PNEUMONIA, and COVID19. Additionally, it is divided into training and testing folders, with three subfolders for each class: NORMAL, PNEUMONIA, and COVID19. The dataset contains a total of 6432 x-ray images, with test data accounting for 20% of the total. Sample data from the dataset's three classes [49] is depicted in Figure 2.6.

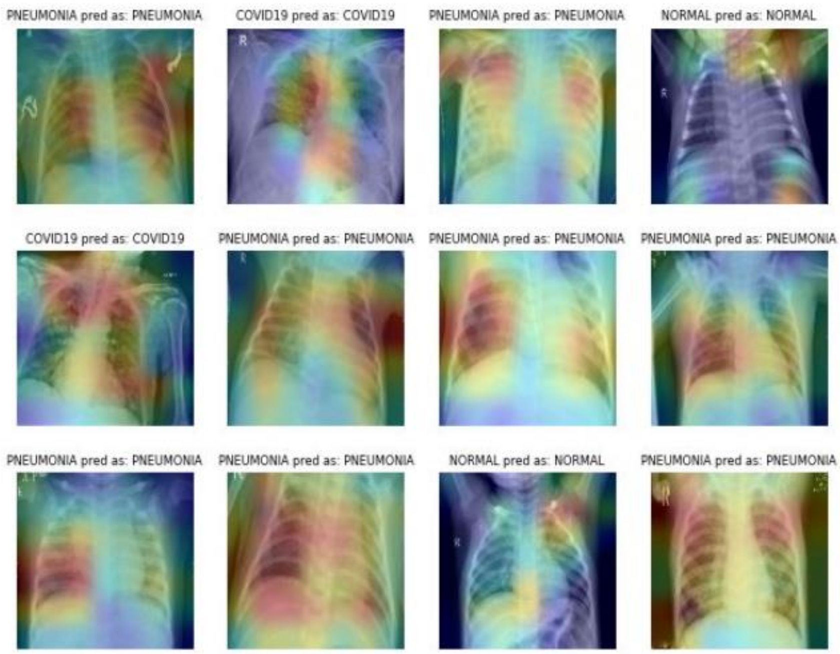

Figure 2.6: Supper Imposed Sample Images for all Three Classes

3. CHAPTER3: METHODOLOGY AND IMPLEMENTATION

3.1 Data Preprocessing

The finalized images are resized and normalized into custom image sizes; here 224 × 224 shapes are used for the resizing technique. Furthermore, the images are fully shuffled in categorical class mode and split into training, validation, and test data as a standard machine learning practice. The training data has 480 images in COVID-19 positive cases, 1266 images in normal cases, and 3418 images in PNEUMONIA cases. Table 3.1 shows the training and testing data distribution among the learning class.

Dataset	COVID-19	PNEUMONIA	NORMAL	Total
Training	480	3418	1266	5164
Testing	116	855	317	1288

Table 3.1: Data set Distribution Among the class

In general, convolutional neural networks (CNN) receive inputs of the same size. All images in the training and testing set need to be resized to a fixed size before feeding them to the convolutional neural networks. And is not required that the input size of the convolutional neural networks should be the same as that of the training data but for consistency standpoint, we used 244 * 244 by image size for the learning process.

3.1.1 Image Augmentation Techniques

Image augmentation is an optimized procedure of altering the existing image data to create more data for the model training process. Additionally, it is the process of synthetically extending the available image dataset for training a deep neural network model. This is extremely helpful when we are proving a data-set with very few data samples. In general, data augmentation strategies can help machine learning models forecast more accurately. Furthermore, for specific image classification issues, a deep learning model with picture augmentation performs better in the training phase in terms of accuracy than a deep learning model without image augmentation.

Cropping, flipping, rotation, scaling, translation, brightness, contrast, color augmentation, saturation, and zooming are all typical image data augmentation techniques. Figure 3.1 shows the X-ray images after the image augmentation. Here we used the zoom range of 0.2 and the rotation range of 15 for data augmentation to enhance the data generalization.

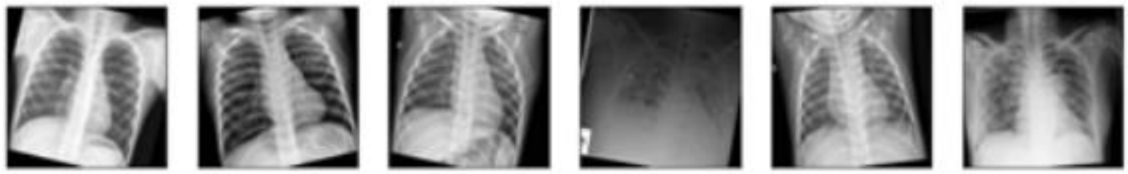

Figure 3.1 X-ray Image sample after Data Augmentation

3.1.2 One-Hot-Encoding

One hot encoding is one method of transforming data to arrange it for an algorithm and get a better and more effective prediction. In general, with one-hot encoding, we transform each categorical value into a new categorical value and designate a binary value of 0 or 1 for those variables. Each integer value is served as a binary vector. Each categorical variable is assigned integer values such as 'COVID19': 0, 'NORMAL': 1, 'PNEUMONIA': 2. Figure 3.2 shows the sample images after the all-data preparation steps.

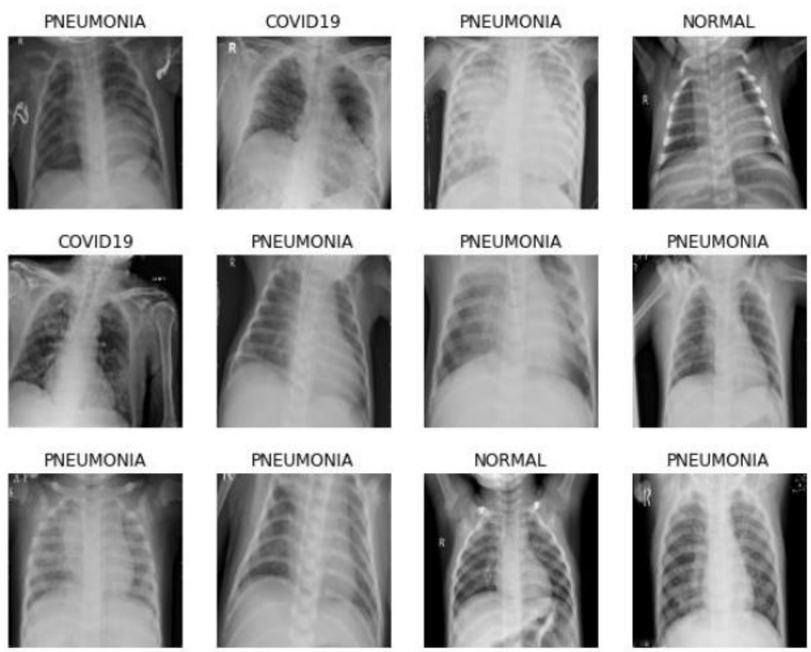

Figure 3.2: X-ray Test Data Set Sample After Data Preparation

3.2 Model Training Procedure

Reduce the learning rate when a metric's performance has plateaued. Most machine learning models benefit from slowing down their learning pace by a factor of 2-10 when learning hibernation. If no improvement is observed after a predetermined number of epochs, this callback option typically monitors a quantity and slows down learning (number of epochs to wait before resuming normal operation after lr has been reduced). Here we use ReduceLROnPlateau to reduce the learning rate when a model metric has stopped improving itself. Furthermore, early stopping is a type of regularization strategy used in machine learning and deep learning to prevent overfitting difficulties while training a machine learning model with an iterative method such as gradient descent. Early Stopping also helps the early stopping of model training via a pre-defined callback called "EarlyStopping." This callback will stop the training process immediately, right after it is triggered.

3.3 Label Smoothing

In one hot encoding, the most critical concern is the hard targets, where the machine learning model tries to generate a logit value for the correct class that is much larger than any of the in-correct classes. However, the incorrect logit values are very distinct from one another. As a result, it will give us a model that is too confident in its predictions during the training process. This may probably lead to over-fitting the model with training data. Instead of keeping the ground truth of one-hot code [0,1,0], we can probably have smoothed code [0.05, 0.9, 0.05], where the alpha value is a hyperparameter for label smoothing (0.1 is a typical value). In general, we have to apply label smoothing when the model is experiencing trouble generalizing or the model is overfitting to the training set. In this study, we use label smoothing techniques to encourage the machine learning model to stay less confident. Instead of reducing cross-entropy with hard targets, we reduce it using soft targets. As a result, it leads to the creation of a better-generalized model for better predictions.

3.4 Treating for Imbalanced Data

When the distribution of samples among the recognized classes is biased or skewed, a classification problem is said to be unbalanced. In other words, the data distribution is uneven or skewed. The data distribution can vary from a slender bias to a very high data imbalance. Imbalanced data presents a barrier for predictive ML modeling, as most machine learning and deep learning algorithms for classification were built on the assumption that each category had a similar number of data samples. This may probably result in machine learning models that have very poor predictive performance in terms of the fewer classes.

In the case where data distribution is considerably different, we can apply a few methods, including class weight. Appling class weight is a basic method that can be used to define data sample weights when fitting the ML classifiers. Table 3.2 shows the data distribution among each class in the COVID-19 X-Ray data set.

Class	Number of Images
NORMAL	1266
PNEUMONIA	3418
COVID19	460

Table 4.2: Table of Training Data Distribution by Class

3.5 Transfer Learning

Transfer learning is a popular machine learning strategy in which a deep learning model produced for one job is utilized as the starting point for a model on a different/sub-task. In general, it is a popular strategy in recent deep learning, where pre-trained machine learning models are used as the starting point for NLP and computer vision processing. If we need to create a model from scratch, it takes a lot of time and computes resources, but here in transfer learning, we can save time and money by using the pre-trained deep learning models instead of developing them from scratch.

The basic purpose of a standard deep learning is to generalize the model for unseen data using patterns identified from the training data. It employs the model generalization process in transfer learning, starting with characteristics or patterns derived from a different task. Rather than starting from the beginning, we must start from patterns that have been established to accomplish a separate subtask, such as classifying X-ray data.

Basic steps for the Transfer Learning

- **Select Source Model:** A pre-trained source machine learning model is selected among the available models. There are a lot of pre-trained models out there, and the best fit model should be selected for our task and accuracy and effectiveness should be considered as core measurements.

- **Re-use the Model:** A pre-trained deep learning model can be used as a starting point for modeling in the second assignment based on the original need. Depending on the modeling strategy used, this may include using the entire ML model or just some of it.

- **Fine Tuning the Model:** Furthermore, the final model could need to be adjusted or improved based on the input-output pair of learning data provided for the task [50].

3.5.1 DenseNet201

To develop our deep learning model in this study, we employed DenseNet201, a densely linked CNN (Convolutional Neural Network). DenseNet201 is a condensed network with 201 layers in which each layer receives cumulative information from the preceding ones. In general, DenseNet201 was designed to resolve the vanishing gradient issue in a convolutional neural network by applying a skip connection. This mechanism is very similar to the ResNet process classification. The main difference between DenseNet and ResNet is: DenseNet concatenates the feature maps that come from the previous layer, whereas ResNet merges the feature maps that come from previous layers. These densely connected patterns lead to a reduced availability of training parameters during the model training.

This is a parametrically improved deep learning model that provides effective results, especially in image classification. DenseNet201 is efficient in memory and resource usage in model training. There are several variations of DenseNet depending on the amount of layers in the neural network. Here in this study, we use DenseNet201 which has 201 layers in the neural network to effectively classify the X-Ray images. Figure 3.3 shows the concatenation process of each presiding layer feature map for creating cumulative knowledge to provide promising results in X-Ray image classification.

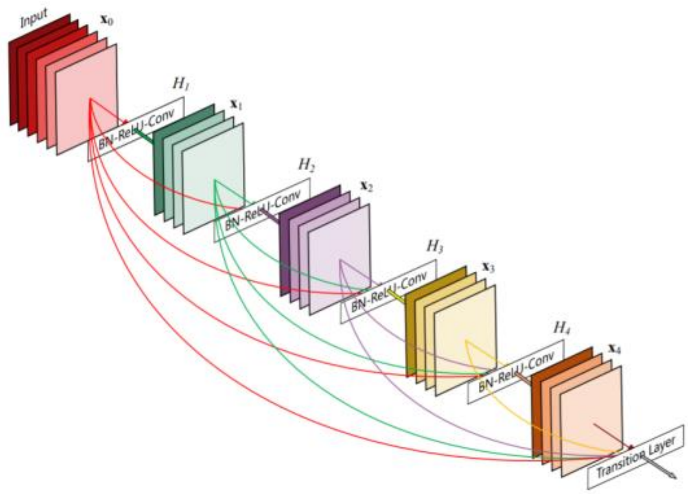

Figure 3.3: High-level Model Network Architecture for DenseNet-201 [51]

The suggested model's convolutional layer is DenseNet-201, which was trained using the COVID-19 X-Ray Images dataset. The COVID-19 X-Ray image dataset is used to train the DenseNet-201 following the high-level procedures listed below.

- To train X-ray images using DenseNet-201 Pre-trained model, using convolution layers, and freezing the model weights before the training process.
- Use 2D (2 dimensional) global average pooling.
- Flatten data.
- Using the ReLU activation function, add X-ray picture data to a dense layer with 64 nodes that is fully connected.
- Transfer data into the connected dense layer, which has three internal nodes, where the COVID-19 image data is classified using the softmax activation function.

In a fully connected dense network, 64 nods are used as the dimensionality of the output space, and Softmax transforms a vector of values into a probability distribution. In general, The final layer of a deep neural network's activation is probably Softmax. The vector values are converted to a probability distribution using a softmax layer with three nodes. In general, Adam is an optimization function for stochastic gradient descent for training deep neural networks. Adam incorporates the best attributes of the RMSProp and AdaGrad algorithms to create an optimization algorithm that can easily manage sparse gradients on noisy data.

Because this COVID-19 X-ray image classification is a multiclass model, the conventional Adam optimizer function and categorical cross entropy loss function were employed. In the designed model, there are 19428163 total parameters, including 1,106,179 trainable parameters and 18,321,984 non-trainable parameters. The training was done with 30 epochs and 16 batches. At epoch 24, the COVID-19 X-ray classification DenseNet-201 model was terminated with a validation accuracy of 0.9554 and a validation loss of 0.3732. It gives 0.9682 accuracy for the DenseNet-201 model.

3.5.2 EfficientNetB7

Google published an innovative paper in 2019 with a new family of CNNs. It is known as the EfficientNet.EfficientNet provides better accuracy as well as improves the efficiency of the deep neural model. It decreases the number of parameters and FLOPS in general (Floating Point Operations Per Second). The key improvements of this study are the design of a basic lightweight baseline architecture (EfficientNet-B0) and the establishment of an effective compound scaling technique for growing the size of the model to get the best accuracy gains. The efficient net model considers the scaling and identifies the balancing of network depth, width, and resolution. These components might help the machine learning model perform better. Based on this discovery, EfficientNet suggests a new model scaling method that use a compound coefficient to uniformly scale nearly all of the width, depth, and resolution parameters. For ImageNet, EfficientNetB7 achieves an improved accuracy of 84.3%. The main point here is that it is 6.1x faster and 8.4x smaller [52].

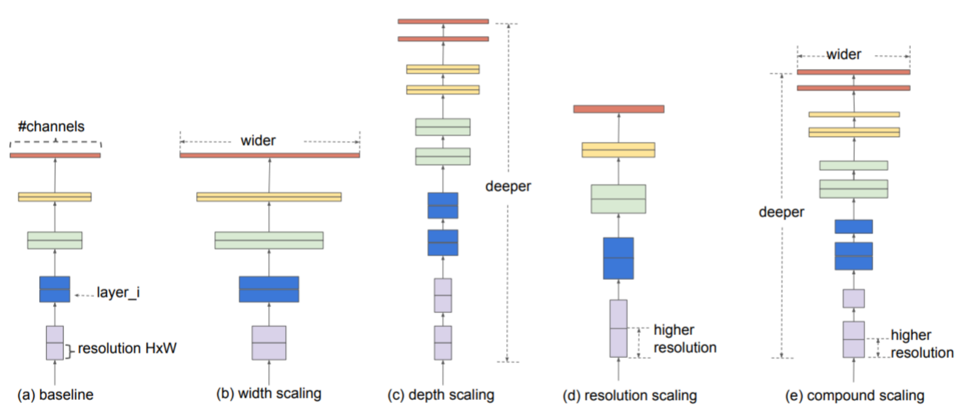

Figure 3.4: The Model's Scaling Structure for EfficientNetB7 Model

Based on this Google study, the EfficientNet architecture proposes a simple but very effective compound scaling approach. Unlike standard practice, which scales these elements inconsistently, the novel architecture adjusts network depth, width, and picture resolution equally using a set of fixed scaling coefficients. When 2Nx times more computational resources are needed, then we can increase the network width by βN, depth by αN, and picture size by γN , where, α, β, γ are constant values defined by a grid search. Furthermore, Figure 3.4 shows the comparison between generic conventional methods and the proposed scaling method.

Stage i	Operator $\hat{\mathcal{F}}_i$	Resolution $\hat{H}_i \times \hat{W}_i$	#Channels $\hat{C}_i$	#Layers $\hat{L}_i$
1	Conv3x3	224×224	32	1
2	MBConv1, k3x3	112×112	16	1
3	MBConv6, k3x3	112×112	24	2
4	MBConv6, k5x5	56×56	40	2
5	MBConv6, k3x3	28×28	80	3
6	MBConv6, k5x5	14×14	112	3
7	MBConv6, k5x5	14×14	192	4
8	MBConv6, k3x3	7×7	320	1
9	Conv1x1 & Pooling & FC	7×7	1280	1

Table 3.3: EfficientNet-B0 Baseline Network Summary Details [44]

EfficientNet-B0 has 237 layers while EfficientNet-B7 has 813 layers in the proposed model. Table 3.3 stresses the kernel size for convolution operations along with the channels, resolution, and layers in the baseline version of EfficientNet-B0. The Macon layer above is related to an inverted bottleneck block with a squeeze and excitation connection added to it. Starting from this B0 baseline architecture, compound scaling can be used to obtain specific EfficientNet B1-B7. Table 3.4 denotes the model performance across all the EfficientNet versions that are improved from the basic baseline EfficientNet-B0 model. The EfficientNet-B7 results showed 84.3% top-level accuracy with 37B FLOPS and 66M total parameters [52].

Model	Top-1 Acc.	Top-5 Acc.	#Params	Ratio-to-EfficientNet	#FLOPs	Ratio-to-EfficientNet
EfficientNet-B0	**77.1%**	**93.3%**	**5.3M**	**1x**	**0.39B**	**1x**
ResNet-50 (He et al., 2016)	76.0%	93.0%	26M	4.9x	4.1B	11x
DenseNet-169 (Huang et al., 2017)	76.2%	93.2%	14M	2.6x	3.5B	8.9x
EfficientNet-B1	**79.1%**	**94.4%**	**7.8M**	**1x**	**0.70B**	**1x**
ResNet-152 (He et al., 2016)	77.8%	93.8%	60M	7.6x	11B	16x
DenseNet-264 (Huang et al., 2017)	77.9%	93.9%	34M	4.3x	6.0B	8.6x
Inception-v3 (Szegedy et al., 2016)	78.8%	94.4%	24M	3.0x	5.7B	8.1x
Xception (Chollet, 2017)	79.0%	94.5%	23M	3.0x	8.4B	12x
EfficientNet-B2	**80.1%**	**94.9%**	**9.2M**	**1x**	**1.0B**	**1x**
Inception-v4 (Szegedy et al., 2017)	80.0%	95.0%	48M	5.2x	13B	13x
Inception-resnet-v2 (Szegedy et al., 2017)	80.1%	95.1%	56M	6.1x	13B	13x
EfficientNet-B3	**81.6%**	**95.7%**	**12M**	**1x**	**1.8B**	**1x**
ResNeXt-101 (Xie et al., 2017)	80.9%	95.6%	84M	7.0x	32B	18x
PolyNet (Zhang et al., 2017)	81.3%	95.8%	92M	7.7x	35B	19x
EfficientNet-B4	**82.9%**	**96.4%**	**19M**	**1x**	**4.2B**	**1x**
SENet (Hu et al., 2018)	82.7%	96.2%	146M	7.7x	42B	10x
NASNet-A (Zoph et al., 2018)	82.7%	96.2%	89M	4.7x	24B	5.7x
AmoebaNet-A (Real et al., 2019)	82.8%	96.1%	87M	4.6x	23B	5.5x
PNASNet (Liu et al., 2018)	82.9%	96.2%	86M	4.5x	23B	6.0x
EfficientNet-B5	**83.6%**	**96.7%**	**30M**	**1x**	**9.9B**	**1x**
AmoebaNet-C (Cubuk et al., 2019)	83.5%	96.5%	155M	5.2x	41B	4.1x
EfficientNet-B6	**84.0%**	**96.8%**	**43M**	**1x**	**19B**	**1x**
EfficientNet-B7	**84.3%**	**97.0%**	**66M**	**1x**	**37B**	**1x**
GPipe (Huang et al., 2018)	84.3%	97.0%	557M	8.4x	-	-

Table 3.4: All EfficientNet Versions Performance Results for ImageNet Dataset [53]

Here in this study, 64 nods are used as the dimensionality of the output space with the ReLU activation function. A SoftMax layer is used with 3 nodes for converting the vector values to a probability distribution. We utilized the Adam optimizer function and the conventional categorical cross-entropy loss function. The intended model has 65,572,499 parameters in total, of which 1,474,819 are trainable and 64,097,680 are not. The training was performed with 30 epochs and a batch size of 16. At epoch 23, the COVID-19 X-ray classification EfficientNet-B7 model was terminated with a validation accuracy of 0.9169 and validation loss of 0.4577. It offers the EfficientNet-B0 model 0.8932 accuracy.

3.5.3 VGG16

For the ImageNet task, the VGG16 model is a lightweight and widely used convolutional neural network (CNN) technique. VGG16 is a massive database object detection project in the computer vision industry. It was developed by Andrew Zisserman and Karen Simonyan at the University of Oxford in 2014. In general, "VGG" stands for "Visual Geometry Group," which is one of the best groups of researchers at Oxford University. In addition to that, "16" indicates that this architecture has 16 neuron layers in the network. In the image net challenge VGG16 deep learning, the model achieved 92.7% accuracy. It improved AlexNet algorithms by extending huge kernel sized filters (one after the other, many 3 × 3 kernel-sized filters). The VGG16 machine learning network is trained for weeks utilizing NVIDIA Titan Black GPUs.

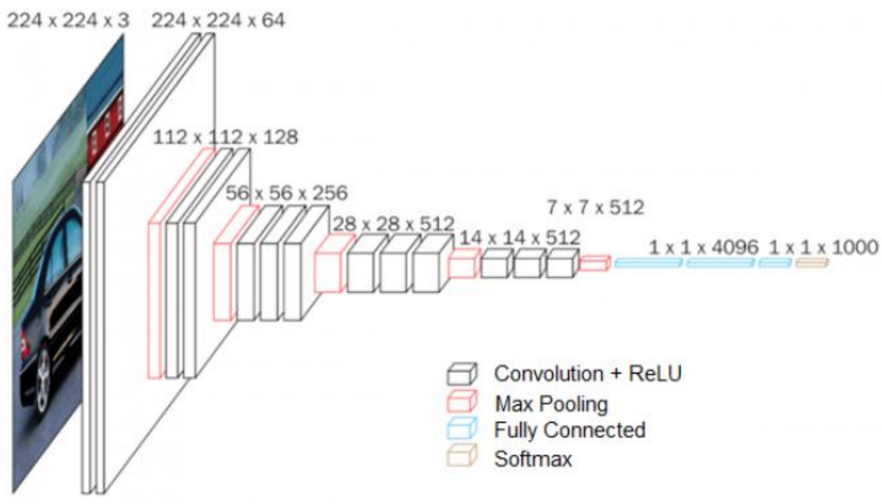

Figure 3.5: The Pre-Trained VGG16 High-level Model Architecture with Layers

Figure 3.5 shows the comprehensive architecture of VGG16 and denotes the Convolution + ReLU, Max Pooling, Fully Connected, and Softmax layers on the neural network lustration. In the VGG16 training procedure, the inputs are fixed to 224*224 RGB images to feed the convolutional nets. It computes the mean RGB value from the training image dataset by considering all the pixels. The image is sent through a few convolutional layers, which have filters with very small responsive 3 × 3 fields. The key advantage is that the VGG16 architecture has fewer parameters and more nonlinearities. The model settings use 1 × 1 filters, which are defined as a linear transformation of the network input channels. The 3 x 3 convolutional layers are added as spatial padding and convolution stride. To ensure that following convolution layers, the spatial resolution is preserved. The activation maps are then transferred over a 2 x 2-pixel frame to the spatial max-pooling layer. This will reduce the size of the activation map to half its original size. At the end of the first stack, the size of the activation map is 112 x 112 x 64. Three fully connected layers follow the model's convolutional layers, with a suitable flattening layer in between the softmax and max-pooling layers, as previously described. While the output layer contains 1,000 neurons associated to the 1,000 classes in the ImageNet dataset, the first and second layers each have 4,096 neurons. Additionally, the softmax activation layer, which supports multiclass categorical categorization, connects to the network output layer [54].

The Keras Applications package is used in this study, together with a transfer learning VGG16 model. The pre-trained model includes the ImageNet associated weights. We can employ core transfer learning ideas to use the pre-trained model. As previously stated, this stack consists of two convolutional layers with 128 filters of size 3 x 3 and ReLU activation. Furthermore, during the training procedure, a 0.5 dropout is employed to drop out the randomly picked neurons. The activation layer for a deep neural network's final layer is likely Softmax. Here, the softmax layer is used with 3 nodes for transforming the vector values into a scattered probability distribution. In general, Adam is an optimization function for stochastic gradient descent for training deep neural networks. Adam combines the best elements of the RMSProp and AdaGrad optimization algorithms to produce a methodology that can easily manage sparse gradients on noisy data. The Adam optimizer function and the customary categorical cross-entropy loss function were used because the COVID-19 X-ray image classification is a multiclass model. There are 15,313,091 total parameters in the planned model, with 598,403 trainable parameters and 14,714,688 non-trainable parameters. The training was done with 30 epochs and 16 batches. After 0.9293 validation accuracy and 0.4241 validation loss, the COVID-19 X-ray classification VGG16 model was stopped at epoch 16. For the VGG16 model, it yields 0.9474 accuracies.

3.5.4 Common System Architecture

Figure 3.6. The inputs come in the form of a human lung image with three sections: COVID-19 positive, pneumonia, and COVID-19 negative people. This suggested system goes through a preprocessing procedure that includes loading X-ray images of a specified size, separating image data, and data augmentation techniques before fitting the deep learning model. As we already know, fine-tuning and fitting the deep learning model improves prediction accuracy. The loss of the model, the confusion matrix, and the model accuracy are all graphically shown to show how loss and accuracy change over time. Finally, in the output portion, the model can predict whether a picture belongs to a COVID-19 patient, normal pneumonia, or COVID -19 negative after the user gives an image as an input.

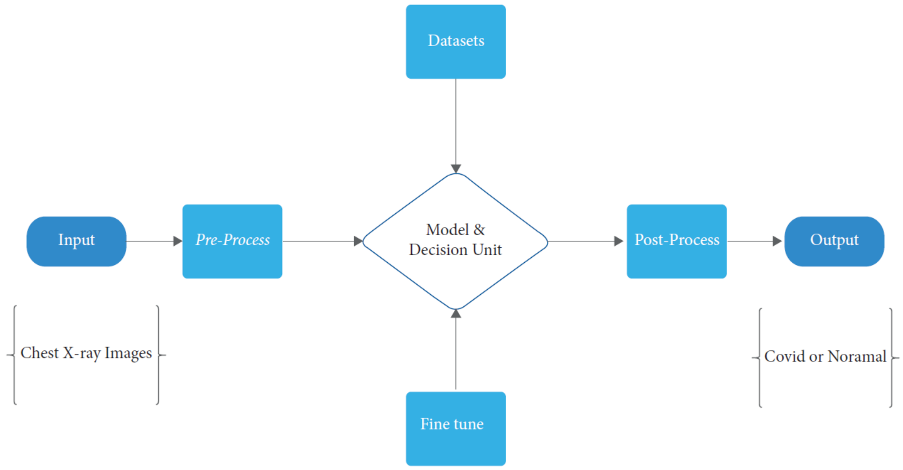

Figure 3.6: High Level Block Diagram for the Pretrained Model Training Process

As shown in Figure 3.7, the system architecture for the pertained deep learning model has four main parts. As we explained in the previous section, the first component involves loading a pre-trained model and the second part involves providing input X-Ray images from the relevant image data set.

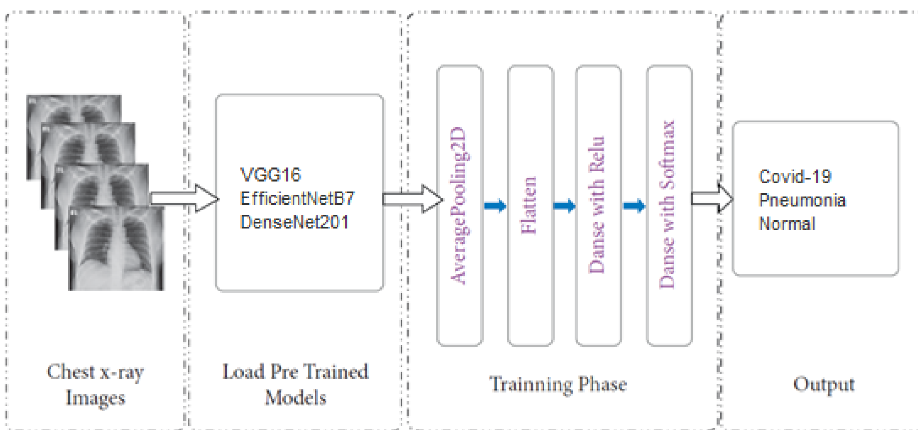

Figure 3.7: Common System Design for the Pre-trained Deep Learning Model

In the second phase, the VGG16, EfficientNetB07, and DenseNet201 deep learning models are loaded. In the third stage, the loaded models were changed using average pooling, flattening, dense with ReLU, and dense with softmax layers. Finally, the data will be reported in the output section as COVID-19-infected, pneumonia, or healthy patients.

3.6 Ensemble Learning

Ensemble learning is an aggregated machine learning procedure that integrates several base machine learning models in order to generate an optimized predictive model. Ensemble learning is basically used to enhance the classification, capabilities of the based models using multiple model capabilities. Here we use a simple averaging stumbling method to take the model average prediction while considering the VGG16, EfficientNetB07, and DenseNet201 models. Figure 3.8 shows the high-level flow diagram of the averaging ensemble technique. The final model will take the average probability of the prediction output of each model and produce the final result based on the average output.

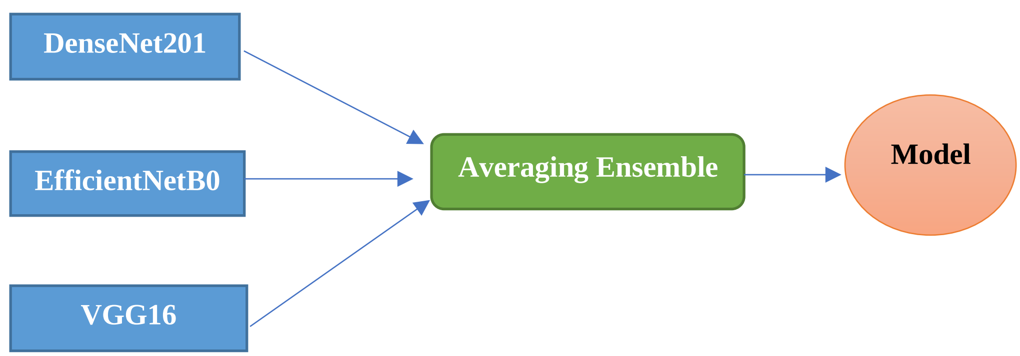

Figure 3.8: Averaging Ensemble Flow Diagram with Based Models

4. CHAPTER 4: EXPERIMENTAL ANALYSIS AND MODEL EVALUATION

4.1 Result and Analysis

4.1.1 Understanding Results through Class Activation Map (CAM)

Class Activation Map (CAM) advanced visualization techniques generate featured heatmaps of two-dimensional class activation on the input images. It indicates how important each part of the image is for the considered class. In general, it allows the image to be classified and understand which parts or pixels of that image have involved more with the final output of the machine learning model.

Figure 4.1: Class Activation Map Images for the COVID-19 Test Sample

As shown in Figure 4.1, the last convolutional neural network layer of the trained network has a size of 7 x 7 x n as its inputs. Therefore, we can find the relevant **heatmap** (7 x 7) and generate the final result as shown above for the COVID19 test sample. It shows which part of the image is mostly involved in the decision-making process.

4.1.2 Understanding Results

Models	Number of Epoch	Accuracy	Validation - Accuracy	Validation Loss
DenseNet-201	24	0.9682	0.9554	0.3732
EfficientNet-B7	23	0.8932	0.9169	0.4577
VGG16	16	0.9474	0.9293	0.4241

Table 4.1: Model Accuracy and High-level Performance Summary

We evaluated the suggested three models to the pretraining deep learning models in order to evaluate them quantitatively. Accuracy, precision, recall, and F1 Score were calculated as four quantitative measures to compare these three models. In contrast to other performance measures, accuracy, precision, and recall provide sufficient information to assess the deep learning model:

$$\text{Accuracy} = \frac{\text{TP} + \text{TN}}{\text{TP} + \text{FP} + \text{FN} + \text{TN}}, \qquad (2)$$

$$\text{Precision} = \frac{\text{TP}}{\text{TP} + \text{FP}}, \qquad (3)$$

$$\text{Recall} = \frac{\text{TP}}{\text{TP} + \text{FN}}. \qquad (4)$$

True positive (TP) and true negative (TN) in Equations (2), (3), and (4) stand in for the correctly named class, whereas false negative (FN) and false positive (FP) stand in for the incorrectly labeled class. If the data's false negative and false positive values are identical, the accuracy is high. Precision is a metric that gauges the quantity of accessible real positive data and counts the number of false positives. The accuracy of the model will also be high if the precision is high. Recall evaluated the false negative values in the data to determine the negative prediction.

As shown in Table 4.1, after training the deep neural models with the validation dataset, the validation accuracy for DenseNet-201, EfficientNet-B0, and VGG16 is 0.9554, 0.9169, and 0.9293, while the validation loss is 0.3732, 0.4577, and 0.4241. DenseNet-201, EfficientNet-B0, and VGG16 provide an accuracy of 0.9682, 0.8932, and 0.9474 for the training dataset. In addition, DenseNet-201, EfficientNet-B0, and VGG16 deep learning models are completed at 24, 23, and 16 epochs during the neural network training process. Figure 4.2 shows the validation accuracy, accuracy, and validation loss for each of the transfer learning models we used in this study.

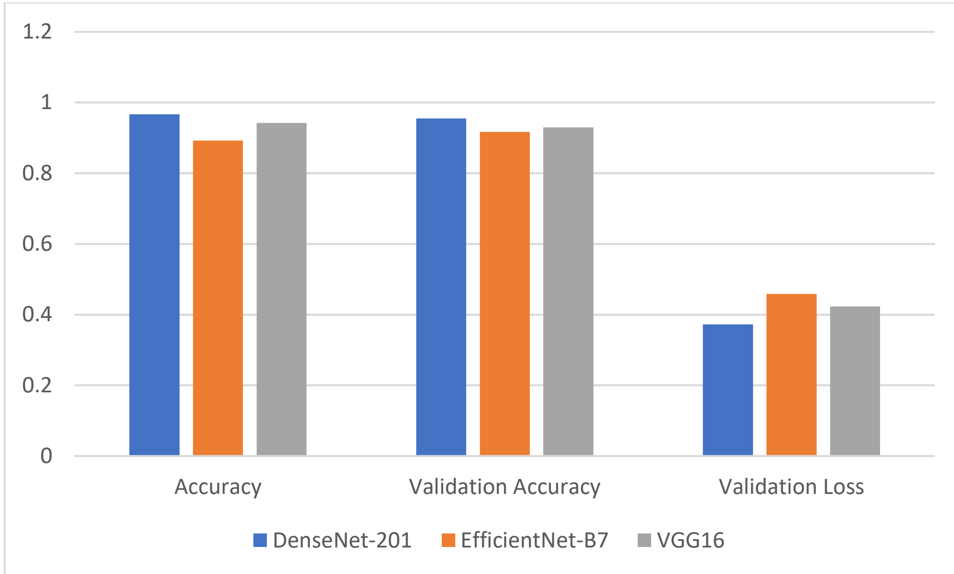

Figure 4.2: Accuracy, Val- Accuracy and Val- Loss Summary for Each Deep Learning Model

Figure 4.3 depicts the DenseNet-201 model's confusion matrix. For the COVID-19, Pneumonia, and healthy classes, the model's accuracy is 0.97, 0.96, and 0.96, respectively. And the recall is for the same class, 0.9, 0.97, and 0.94. In addition, the F1 scores for the three classes mentioned above are 0.88, 0.97, and 0.93. Figure 4.4 shows the performance summary of DenseNet-201. Finally, the Macro-F1 score for DenseNet-201 is 0.92. In addition, Figure 4.5 shows the sample test results for DenseNet-201, and this illustration has both the predicted label and the actual label on top of the respective X-ray image.

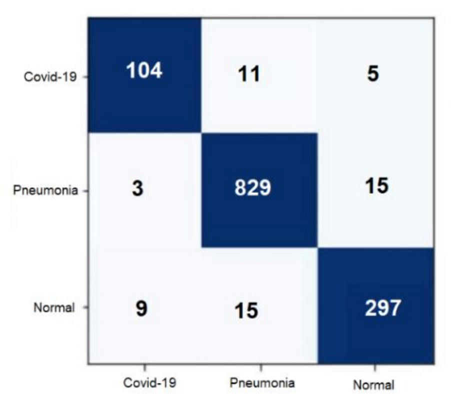

Figure 4.3: Confusion Matrix for DenseNet-201 Model

Class	n (truth)	n (classified)	Accuracy	Precision	Recall	F1 Score
1	116	120	97.83%	0.87	0.90	0.88
2	855	847	96.58%	0.98	0.97	0.97
3	317	321	96.58%	0.93	0.94	0.93

Figure 4.4: Performance Summary for DenseNet-201 Model

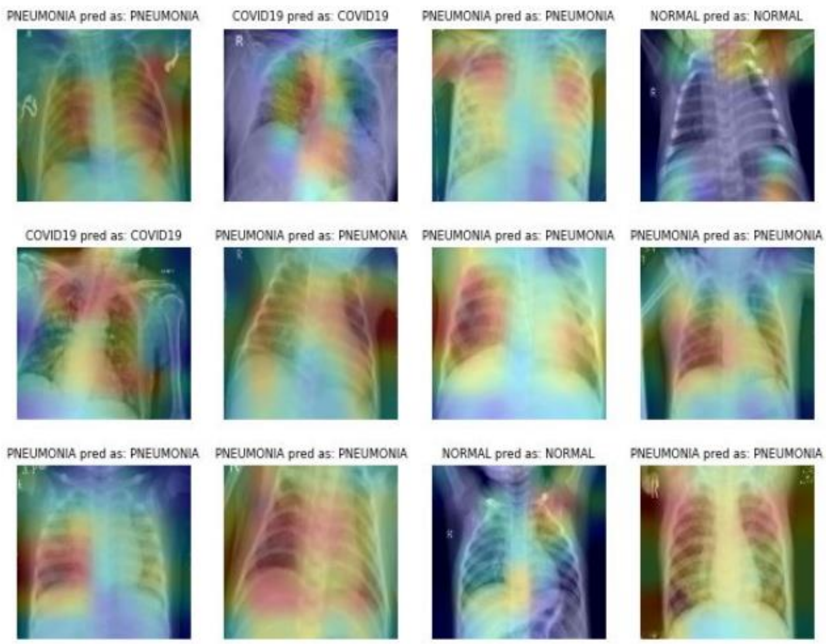

Figure 4.5: Sample Test Result for DenseNet-201 Model

Figure 4.6 depicts the EfficientNet-B7 model's confusion matrix. The Covid-19 Positive, Pneumonia, and Negative classes have model precisions of 0.74, 0.95, and 0.90, respectively. And the recall for the same classes is 0.7, 0.96, and 0.88. In addition, the F1 scores for the above three classes are 0.72, 0.95, and 0.89. Figure 4.7 shows the performance summary of **EfficientNet-B7**. Finally, the Macro-F1 score for **EfficientNet-B7** is 0.8533. Figure 4.8 shows the sample test results for **EfficientNet-B7** and this illustration has the predicted label and the actual label on top of the respective X-ray image.

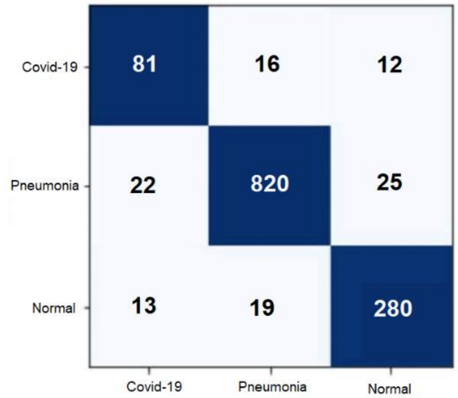

Figure 4.6: Confusion Matrix for EfficientNet-B7 Model

Class	n (truth)	n (classified)	Accuracy	Precision	Recall	F1 Score
1	116	109	95.11%	0.74	0.70	0.72
2	855	867	93.63%	0.95	0.96	0.95
3	317	312	94.64%	0.90	0.88	0.89

Figure 4.7: Performance Summary for EfficientNet-B7 Model

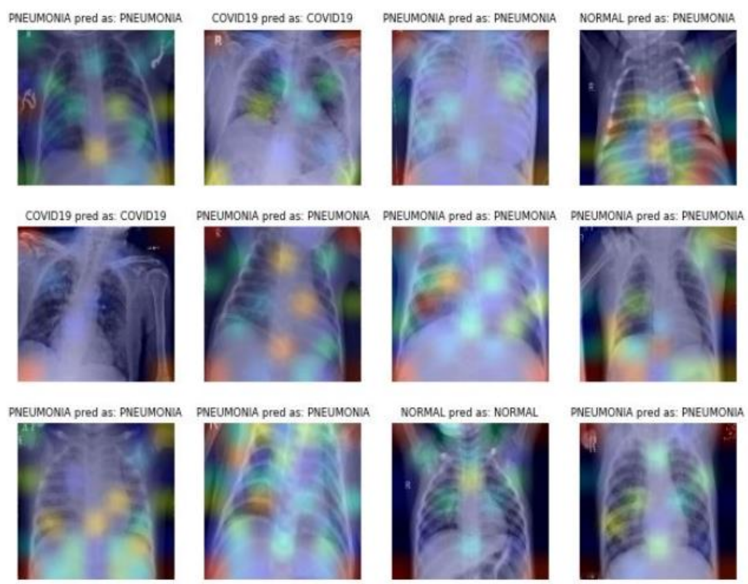

Figure 4.8: Sample Test Result for EfficientNet-B7 Model

The VGG16 model's confusion matrix is shown in Figure 4.9. The precision of the model for COVID-19, pneumonia, and the normal class is 0.79, 0.95, and 0.91. And the recall for the same classes was 0.78, 0.96, and 0.89. In addition, the F1 scores for the above three classes are 0.78, 0.96, and 0.90. Figure 4.10 shows the performance summary of VGG16. Finally, the Macro-F1 score for VGG16 is 0.88. Figure 4.11 depicts the sample test results for VGG16, with the expected and real labels superimposed on top of the corresponding X-ray picture.

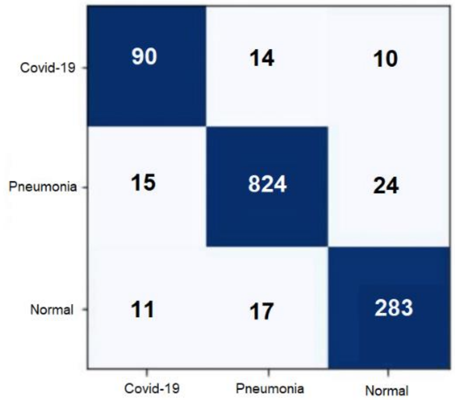

Figure 4.9: Confusion Matrix for VGG16 Model

Class	n (truth)	n (classified)	Accuracy	Precision	Recall	F1 Score
1	116	114	96.12%	0.79	0.78	0.78
2	855	863	94.57%	0.95	0.96	0.96
3	317	311	95.19%	0.91	0.89	0.90

Figure 4.10: Performance Summary for VGG16 Model

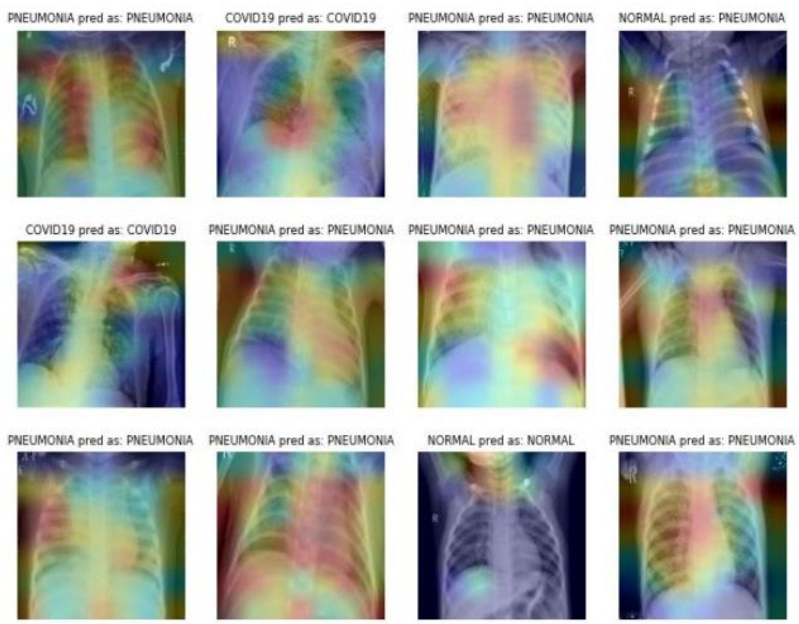

Figure 4.11: Sample Test Result for VGG16 Model

The three models are combined and created into one single model. The ensemble model completed all the given 7 epochs and stopped with a 0.9596 validation accuracy and a 0.1407 validation loss. The accuracy for the ensemble model is 0.9667. Based on Table 4.2, we identified that many studies are done with two classes in the training X-ray dataset. VGG19, ResNet50, ResNetV2, and InceptionV3 have commonly used methods in terms of the model architecture. In the past studies, we could not find any related studies done for EfficientNet-B7. However, based on Table 4.2, the highest accuracy of 96.78 is reported by MobileNetV2.In our study, three models were used for the performance analysis, with the highest accuracy of 95.54 reported by DenseNet-201. It is the second-largest accuracy for three class scenarios using the chest x-ray image data.

#Image samples	Class	Architectures	Best Performing Architecture	Performanc e/ Accuracy %	Recall %	Precision %	Refer ence
1428	3	VGG19, MobileNetV2, Inception, Xception, InceptionResNet V2	MobileNetV2	96.78	98.66	96.46	[55]
204	2	Resnet50	Resnet50 + custom CNN	98.1	96.2	98.7	[56]
100	2	ResNet50, InceptionV3, InceptionRes-NetV2	ResNet50	98	86.1	98.6	[57]
21,152	2	CNN	CNN	94.64	96.5	92.86	[58]
13,975	2	COVID-CAPS	COVID-CAPS	95.7	90	95.8	[59]
400	2	InceptionResNet V2, ResNet50, VGG19, MobilenetV2, NasNetMobile, ResNet15V2	NasNetMobil e	93.94	95	95	[60]
75	2	VGG19, Xception, ResNetV2, DenseNet, InceptionV3,	VGG19, DenseNet	91	91	93	[61]

		MobileNetV2, InceptionResNet V2					
1127	2	Modified Darknet	Modified Darknet	98.08	95.13	98.03	[62]
7470	2	MD-Conv	MD-Conv	98.3	96.8	94.1	[63]
380	2	Novel CNN Model, ResNet50	ResNet50	92.6	88.00	97.78	[64]
1257	3	Xception	Xception	84	91	77	[65]
6,452*	3	DenseNet-201, EfficientNet-B7, VGG16	DenseNet-201	95.54	93.66	92.66	This study

Table 4.2: COVID-19 Ease Detection Performance Summary of Previous Studies Using Deep Learning

Model	**Accuracy**	**Precision**	**Recall**	**F1 Score**
DenseNet-201	0.9554	0.9266	0.9366	0.9266
EfficientNet-B7	0.9169	0.8633	0.8466	0.8533
VGG16	0.9293	0.8833	0.8766	0.88

Table 4.3: Model Accuracy, Precision, Recall and F1 Score Summary for All Three Modes

The following sensitivity values are given for the Densenet201, EfficientNet07, and VGG16 models: 0.9366, 0.8466, and 0.8766. For the X-ray image data set, Densenet201 has been reported to have the maximum sensitivity and accuracy. All three of the comparable models, 0.9266, 0.8633, and 0.8833, depend heavily on average precision. According to Table 4.3, the average F1 Scores for the aforementioned three models are 0.9266, 0.8533, and 0.88.

5. CHAPTER 5: DISCUSSION AND CONCLUSION

5.1 Discussion

The SARS-CoV-2-related COVID-19 virus is spreading quickly around the world. Stages like X-ray` imaging, clinical observations, and nucleic acid screening are completed for the diagnosis of COVID-19. It is crucial that COVID-9 detection and infected patients can be under control as soon as feasible on a global scale. Deep learning-based systems are being built on X-ray images for this purpose. This paper proposes automated deep learning methods for COVID-19 diagnosis from X-ray images. For categorizing X-ray images, we provided pre-trained CNN models such as DenseNet-201, EfficientNet-B7 and VGG16.

In general, when the COVID-19 virus enters the human body, it has an immediate effect on the mucosal membrane. Most of the time, the mucus membrane contacts all of the parts of the respiratory system, such as the nose, mouth, eyes, and lungs. As we already know, the virus attacks healthy cells and uses them to create a new virus. This procedure takes place in either the upper or lower respiratory system. Most of the time, it travels down in human airways. The virus infects a healthy cell, which it then uses to spread itself. It replicates and spreads new viruses to nearby cells. Both the top and bottom respiratory tracts can be infected by the novel coronavirus. It passes through your lungs. As part of this process, the lining can be inflamed and irritated. In addition, the virus infection can come out from underneath into human alveoli. Around 80% of patients who have COVID-19 get infected with moderate to mild symptoms. They may have a slight sore throat or a savior dry cough. Doctors can diagnose signs of human respiratory inflammation on a lung CT scan or X-ray. Using the X-ray images, medical practitioners can check the "ground-glass opacity" in the patient's lungs (frosted glass on a lung shower door) [66]. Performance data reveals that among the various deep learning models, the Densenet201 pre-trained model produced the greatest accuracy of 95.54 % and precision of 92.66 %. Other deep learning models are contrasted with this one. The comparison analysis shows that Densenet201 outperforms the other deep learning techniques. Therefore, the technique is applicable to disease diagnosis. In this study, three based models are employed to increase overall accuracy utilizing the ensemble approach. Accuracy of the ensemble model is 0.9667. The accuracy of this is superior to that of Densenet201.

According to these investigations, the COVID-19 virus directly affects human lungs in the early stages of infection, and X-Ray images can be utilized to diagnose the virus infection by utilizing "ground-glass opacity." Therefore, we can use the proposed deep learning model with 95.54% accuracy to detect the COV-19 virus in the patient's respiratory system. How well a machine learning model can identify positive examples is measured by its sensitivity. The true positive rate (TPR) or recall are other names for it.

Because it enables us to observe how many positive examples the model was able to correctly detect, sensitivity is used to assess model performance. Sensitivity results for the Densenet201, VGG16, and EfficientNet07 models are presented as follows: 0.9366, 0.88, and 0.8466. Densenet201 is reported the highest sensitivity as well as the highest accuracy for the X-ray image data set.

5.2 Conclusion

To obtain the claimed accuracy, this study used the pre-trained DenseNet-201, EfficientNet-B7, and VGG16 models, which were changed in the final layer. There are 6,452 COVID-19 Positive, Pneumonia, and Normal pictures in the COVID-19 dataset. The accuracy of the DenseNet-201, EfficientNet-B7 and VGG16 models is 0.9554, 0.9169, and 0. 9293. The highest value of 0.9554 is reported by the DenseNet-201 model. Extensive additional research will be conducted on a more balanced and larger X-Ray dataset, as well as with various transfer learning architectures.

X-ray image feature extraction and classification are performed well. Each of the three models checked produced the expected results. The COVID-19 virus may be detected using a simple X-Ray image using the DenseNet-201, EfficientNet-B7, and VGG16 models in a short amount of time. X-ray equipment is, in general, readily available and extremely cost-effective for patients. It has the potential to be a quite proper and effective tool for identifying people who are infected with COVID-19. This proposed approach for detecting and tracking the COVID-19 virus is quick, and there is little risk of the virus spreading during the pandemic if you wait to test for it. In training, a variety of data augmentation techniques were employed to prevent overfitting on the test set. Additionally, the final model's weights were based on the model's accuracy performance on the validation data, which was the best. To further prevent the model from overfitting, dropout regularization was implemented.

5.3 Limitation

In general, X-rays are a type of electromagnetic radiation that occurs naturally. When sufficiently energetic charged particles impact a substance, they are produced. The effects of utilizing X-rays on the human body have drawn significant concern from researchers in recent decades. In addition to other temporary adverse effects such bleeding, dizziness, vomiting, hair loss, skin loss, etc., the danger of developing cancer is incredibly minimal [67].

"Natural Background Radiation" (NBR) is the radiation that surrounds nature at all times. The NBR mainly originates from thoron and radon in the natural air, from natural occurrences in drinks and food, buildings and soil, and space. However, the natural background radiation (NBR) level is approximately 4.1 millisieverts per year (mSv/yr), but this value differs from situation to situation. However, based on previous studies, the effective dose is < 0.1 mSv and the insignificant risk is less than 1 in 1,000,000 [68].

5.4 Future Works

The study's next work will be focused on improving the suggested system's clinical acceptability and accuracy. The ability to seamlessly integrate the feedback of the physiologist and radiologist with the automated system could aid in the development of a reliable diagnostic system. Furthermore, a detailed analysis of the performance differences between classical algorithms and deep learning methods could aid in the implementation of clinical acceptability.

However, the ensemble architecture failed to provide correct predictions in numerous circumstances, as previously indicated. In the future, we may perform more research into sophisticated strategies for improving image quality, such as X-ray picture contrast augmentation or additional processing stages. We might also consider segmenting lung images before identifying them in order to optimize the CNN network's feature extraction process. Furthermore, advanced technologies such as snapshot assembling could be used in the future to reduce processing requirements and resources.

REFERENCES

[1] WorldOmter, COVID-19 CORONAVIRUS PANDEMIC, American Library Association,2021, [Online], https://www.worldometers.info/coronavirus/

[2] K. Sharma, Coronavirus: Distressed Breathing, Lung Involvement in COVID Here's What Doctors Want You to Know—Times of India, +e Times of India, Bombay, India, 2021, https://timesofindia.indiatimes.com/life-style/healthfitness/health-news/coronavirus-distressed-breathing-lunginvolvement-in-covid-heres-what-doctors-want-you-to-know/articleshow/82195455.cms.

[3] Z. KARHAN and F. AKAL, "Covid-19 Classification Using Deep Learning in Chest X-Ray Images," 2020 Medical Technologies Congress (TIPTEKNO), 2020, pp. 1-4, doi: 10.1109/TIPTEKNO50054.2020.9299315.

[4] Wang W, Xu Y, Gao R, Lu R, Han K, Wu G, Tan W. Detection of SARS-CoV-2 in Different Types of Clinical Specimens. JAMA. 2020 May 12;323(18):1843-1844. doi: 10.1001/jama.2020.3786. PMID: 32159775; PMCID: PMC7066521.

[5] Ming-Yen Ng, Elaine Y. P. Lee, Jin Yang, Fangfang Yang, Xia Li, Hongxia Wang, Macy Mei-sze Lui, Christine Shing-Yen Lo, Barry Leung, Pek-Lan Khong, Christopher Kim-Ming Hui, Kwok-yung Yuen, Michael D. Kuo, "Imaging Profile of the COVID-19 Infection: Radiologic Findings and Literature Review",2020 Feb 13, Cardiothoracic Imaging 2020; pp. 4 https://doi.org/10.1148/ryct.2020200034.

[6] Sharmila V J, Jemi Florinabel D, "Deep Learning Algorithm for COVID-19 Classification Using Chest X-Ray Images", Computational and Mathematical Methods in Medicine, vol. 2021, Article ID 9269173, pp. 1, 2021. https://doi.org/10.1155/2021/9269173.

[7] Nguyen D, Kay F, Tan J, Yan Y, Ng YS, Iyengar P, Peshock R, Jiang S. Deep Learning-Based COVID-19 Pneumonia Classification Using Chest CT Images: Model Generalizability. Front Artif Intell. 2021 Jun 29; pp. 2. doi: 10.3389/frai.2021.694875. PMID: 34268489; PMCID: PMC8275994.

[8] Ali, R.M.M., Ghonimy, M.B.I. Radiological findings spectrum of asymptomatic coronavirus (COVID-19) patients. Egypt J Radiol Nucl Med 51,156 (2020),pp.1, https://doi.org/10.1186/s43055-020-00266-3.

[9] Akter S, Shamrat FMJM, Chakraborty S, Karim A, Azam S. COVID-19 Detection Using Deep Learning Algorithm on Chest X-ray Images. Biology (Basel). 2021 Nov 13; pp. 1, doi: 10.3390/biology10111174. PMID: 34827167; PMCID: PMC8614951.

[10] Teymouri M, Mollazadeh S, Mortazavi H, Naderi Ghale-Noie Z, Keyvani V, Aghababaei F, Hamblin MR, Abbaszadeh-Goudarzi G, Pourghadamyari H, Hashemian SMR, Mirzaei H. Recent advances and challenges of RT-PCR tests for the diagnosis of COVID-19. Pathol Res Pract. 2021 May; pp.2. doi: 10.1016/j.prp.2021.153443. Epub 2021 Apr 14. PMID: 33930607; PMCID: PMC8045416.

[11] Dilbag S, Kumar V, Vaishali, Kaur M. Classification of covid-19 patients from chest CT images using multi-objective differential evolution–based convolutional neural networks. Eur J Clin Microbiol Infect Dis 2020:1–15. https:// doi.org/10.1007/s10096-020-03901-z.

[12] Y. Pathak a, P.K. Shukla b, A. Tiwari c, S. Stalin d, S. Singh e, P.K. Shukla f, Deep Transfer Learning Based Classification Model for COVID-19 Disease, Elsevier Masson SAS on behalf of AGBM, 2020: PP 1-3.

[13] Choi H, Qi X, Yoon SH, Park SJ, Lee KH, Kim JY, et al. Extension of coronavirus, disease 2019 (covid-19) on chest CT and implications for chest radiograph interpretation. Radiol Card Imaging 2020;2(2): e 2001-07.

[14] Panagis Galiatsatos, M.D., M.H.S., Johns Hopkins Bayview Medical Center, online: https://www.hopkinsmedicine.org/health/conditions-and-diseases/coronavirus/what-coronavirus-does-to-the-lungs, 2021.

[15] Jonathan Shadwell, Rediopaedia, online: https://radiopaedia.org/articles/acute-respiratory-distress-syndrome-1, 2021.

[16] Sanjay N Jain, Tanvi Modi, Yashant Aswani, and Ravi U Varma1 , “Chest radiography in adult critical care unit: A pictorial review”, PMC, 2019 OCT ,PP 418–425.

[17] Carrillo-Bayona J.A., Arias-Alvarez L. (2018) Diagnostic Imaging in Sepsis of Pulmonary Origin. In: Ortiz-Ruiz G., Dueñas-Castell C. (eds) Sepsis. Springer, New York, NY. https://doi.org/10.1007/978-1-4939-7334-7_5.

[18] Hyun Jung Koo, Soyeoun Lim, Jooae Choe, Sang-Ho Choi, Heungsup Sung, Kyung-Hyun Do , 'Radiographic and CT Features of Viral Pneumonia',Radiographic, Online : https://doi.org/10.1148/rg.2018170048 , 2018.

[19] Zhang K. & Goldbaum M. Labeled Optical Coherence Tomography (OCT) and Chest XRay Images for Classification. (Mendeley,2018).

[20] Kundu R, Das R, Geem ZW, Han G-T,Sarkar R (2021) Pneumonia detection in chest Xray images using an ensemble of deep learning models. PLoS ONE 16(9): e0256630. https://doi.org/10.1371/journal.pone.0256630.

[21] Islam, M.M. Karray, F.; Alhajj, R.; Zeng, J. A Review on Deep Learning Techniques for the Diagnosis of Novel Coronavirus (COVID-19). IEEE Access 2021, 9, 30551–30572. [CrossRef] 9. Alafif, T.; Tehame, A.M.

[22] Bajaba, S.; Barnawi, A.; Zia, S. Machine and Deep Learning towards COVID-19 Diagnosis and Treatment: Survey, Challenges, and Future Directions. Int. J. Environ. Res. Public Health 2021, 18, 1117. [CrossRef].

[23]Alafif, T.; Tehame, A.M.; Bajaba, S.; Barnawi, A.; Zia, S. Machine and Deep Learning towards COVID-19 Diagnosis and Treatment: Survey, Challenges, and Future Directions. Int. J. Environ. Res. Public Health 2021, 18, 1117. [CrossRef].

[24] F. Shan, Y. Gao, J. Wang et al., "Lung infection quantification of covid-19 in ct images with deep learning," 2020, https:// arxiv.org/abs/2003.04655.

[25] S. Wang, B. Kang, J. Ma et al., "A deep learning algorithm using ct images to screen for corona virus disease (COVID19)," European Radiology, vol. 31, 2020.

[26] C. Zheng, Deep Learning-Based Detection for COVID-19 from Chest CT Using Weak Label, medRxiv, Cold Spring, NY, USA, 2020.

[27] Azher Uddin ,Bayazid Talukder ,Mohammad Monirujjaman Khan ,Atef Zaguia , Study on Convolutional Neural Network to DetectCOVID-19 from Chest X-Rays, Mathematical Problems in Engineering, VOL : 2021 , 2021 .PP 3.

[28] Azher Uddin ,Bayazid Talukder ,Mohammad Monirujjaman Khan ,Atef Zaguia , Study on Convolutional Neural Network to DetectCOVID-19 from Chest X-Rays, Mathematical Problems in Engineering, VOL : 2021 , 2021 .PP 4.

[29] Anand R, Sowmya V, Vijaykrishnamenon, E.A. Gopalakrishnan K.P. soman, MODIFIED VGG DEEP LEARNING ARCHITECTURE FOR COVID-19 CLASSIFICATION USING BIO-MEDICAL IMAGES, IOP Conf. Series: Materials Science and Engineering,2001, 2-5.

[30] Nardelli P, Jimenez-Carretero D, Bermejo-Pelaez D, Washko GR, Rahaghi FN,Ledesma-Carbayo MJ, et al. Pulmonary artery–vein classification in CT images using deep learning. IEEE Trans Med Imaging 2018;37(11):2428–40.

[31] Q. Li, W. Cai, X. Wang, Y. Zhou, D. D. Feng, and M. Chen,"Medical image classification with convolutional neural network," in Proceedings of the 13th International Conference on Control Automation Robotics & Vision (ICARCV), pp. 844–848, Singapore, December 2014.

[32] S. Wang, B. Kang, J. Ma et al., "A deep learning algorithm using ct images to screen for corona virus disease (COVID- 19)," European Radiology, vol. 31, 2020.

[33] Y. Pathak a, P.K. Shukla b, A. Tiwari c, S. Stalin d, S. Singh e, P.K. Shukla f ,Deep Transfer Learning Based Classification Model for COVID-19 Disease, Elsevier Masson SAS on behalf of AGBM, 2020: PP 2-4.

[34] Badawi, A.; Elgazzar, K. Detecting Coronavirus from Chest X-rays Using Transfer earning.COVID 2021, 1, 403–415. https://doi.org/10.3390/covid1010034

[35] Dongsheng Ji ,Zhujun Zhang ,Yanzhong Zhao , Qianchuan Zhao1, Research on Classification of COVID-19 Chest X-Ray ImageModal Feature Fusion Based on Deep Learning, Journal of Healthcare Engineering, Volume 2021, Article ID 6799202, 12 pages, 2021,PP 6-7.

[36] Shoeibi, A. et al. Automated detection and forecasting of COVID-19 using deep learning techniques: A review. arXiv preprint arXiv:2007.10785 (2020).

[37] D. Apostolopoulos and T. A. Mpesiana, “Covid-19: automatic detection from X-ray images utilizing transfer learning with convolutional neural networks,” Physical and Engineering Sciences in Medicine, vol. 43, no. 2, pp. 635–640, 2020.

[38] Sahinbas and F. O. Catak, “Transfer learning-based convolutional neural network for COVID-19 detection with X-ray images,” in Data Science for COVID-19Elsevier, Amsterdam, Netherland, 2021.

[39] Rajpurkar P., et al. , “CheXNet: radiologist-level pneumonia detection on chest x-rays with deep learning,” arXiv abs/1711.05225 (2017).

[40] Jenita Manokaran, Fatemeh Zabihollahy,b Andrew Hamilton-Wright,c and Eranga Ukwattaa,Detection of COVID-19 from chest x-ray images using transfer learning, J Med Imaging (Bellingham). 2021 Jan ,Vol 8

[41] M. E. H. Chowdhury, T. Rahman, A. Khandakar et al., “Can AI help in screening viral and COVID-19 pneumonia?” vol. 8, pp. 132665–132676, 2020.

[42] Jenish Maharjan, Jacob Calvert, Emily Pellegrini, Abigail Green-Saxena, Jana Hoffman, Andrea McCoy, Qingqing Mao, Ritankar Das,Application of deep learning to identify COVID-19 infection in posteroanterior chest X-rays,Clinical Imaging,Volume 80,2021,Pages 268-273,

[43] E. E.-D. Hemdan, M. A. Shouman, and M. E. J. A. P. A. Karar, Covidx-Net: A Framework of Deep Learning Classifiers to Diagnose Covid-19 in X-Ray Images, MedRxiv, Cold Spring, NY, USA, 2020.

[44] Vardan Agarwal, Complete Architectural Details of all EfficientNet Models, toword data science,2020,[online],https://towardsdatascience.com/complete-architectural-details-of-all-efficientnet-models-5fd5b736142.

[45] Vinayakumar Ravi1, Harini Narasi, Chinmay Chakraborty3, Tuan D. Pham1, Deep learning-based meta-classifer approach for COVID-19 classifcation using CT scan and chest X-ray images, Center for Artifcial Intelligence, Prince Mohammad Bin Fahd University, Khobar, Saudi Arabia, 2021 PP. 5-12.

[46] Kundu R., Basak H., Singh P., Ahmadian A., Ferrara M. & Sarkar R. Fuzzy rank-based fusion of CNN models using Gompertz function for screening COVID-19 CT-scans. Scientific Reports. 11, 14133 (2021,7), https://doi.org/10.1038/s41598-021-93658-y PMID: 34238992.

[47] Gabruseva T., Poplavskiy D. & Kalinin A. Deep learning for automatic pneumonia detection. Proceedings of the IEEE/CVF Conference on Computer Vision and Pattern Recognition Workshops. pp. 350- 351 (2020).

[48] Kundu R, Das R, Geem ZW, Han G-T, Sarkar R (2021) Pneumonia detection in chest Xray images using an ensemble of deep learning models. PLoS ONE 16(9): e0256630. https://doi. org/10.1371/journal.pone.0256630.

[49] Ibrahim Sobh, Chest X-ray (Covid-19 & Pneumonia) , Kaggle, 2019, Available online : https://www.kaggle.com/datasets/prashant268/chest-xray-covid19-pneumonia.

[50] Jason Brownlee , A Gentle Introduction to Transfer Learning for Deep Learning ,Deep Learning for Computer Vision , 2017 Online: https://machinelearningmastery.com/transfer-learning-for-deep-learning/.

[51] Huang, Gao, et al. “Densely Connected Convolutional Networks.” ArXiv , 25 Aug. 2016, pp. 1–1., arxiv.org/abs/1608.06993.

[52] Mingxing Tan, Quoc V. Le, Efficient Net: Rethinking Model Scaling for Convolutional eural Networks, V5, International Conference on Machine Learning, Long Beach, California, PMLR 97, 2019. pp. 1- 8.

[53] Mingxing Tan, Quoc V. Le, Efficient Net: Rethinking Model Scaling for Convolutional eural Networks, V5, International Conference on Machine Learning, Long Beach, California, PMLR 97, 2019. pp. 6- 8.

[54] Tinsy John Perumanoor , What is VGG16? — Introduction to VGG16 ,Great Learning , 2020, [Online] https://medium.com/@mygreatlearning/what-is-vgg16-introduction-to-vgg16-f2d63849f615.

[55] 35. Apostolopoulos, I.D.; Mpesiana, T.A. Covid-19: Automatic detection from X-ray images utilizing transfer learning with convolutional neural networks. Phys. Eng. Sci. Med. 2020, 43, 635–640.

[56] Hall, L.O.; Paul, R.; Goldgof, D.B.; Goldgof, G.M. Finding Covid-19 From Chest X-Rays Using Deep Learning on a Small Dataset. arXiv 2020, arXiv:2004.02060. Available online: http://arxiv.org/abs/2004.02060 (accessed on 15 August 2021).

[57] Narin, A. Kaya, C. Pamuk, Z. Automatic detection of coronavirus disease (COVID-19) using X-ray images and deep convolutional neural networks. Pattern Anal. Appl. 2021, 24, 1207–1220.

[58] Tang, Y.-X.; Tang, Y.-B.; Peng, Y.; Yan, K.; Bagheri, M.; Redd, B.A.; Brandon, C.J.; Lu, Z.; Han, M.; Xiao, J.; et al. Automated abnormality classification of chest radiographs using deep convolutional neural networks. NPJ Digit. Med. 2020, 3, 1–8.

[59] Afshar, P.; Heidarian, S.; Naderkhani, F.; Oikonomou, A.; Plataniotis, K.N.; Mohammadi, A. COVID-CAPS: A capsule networkbased framework for identification of COVID-19 cases from X-ray images. Pattern Recognit. Lett. 2020, 138, 638–643.

[60] Ahsan, M.; Gupta, K.; Islam, M.; Sen, S.; Rahman, L.; Hossain, M.S. COVID-19 Symptoms Detection Based on NasNetMobile with Explainable AI Using Various Imaging Modalities. Mach. Learn. Knowl. Extr. 2020, 2, 490–504.

[61] Hemdan, E.E.; Shouman, M.A.; Karar, M.E. COVIDXnet: A framework of deep learning classifiers to diagnose COVID-19 in X-ray images. arXiv 2020, arXiv:2003.11055. Available online: http://arxiv.org/abs/2003.11055 (accessed on 19 August 2021).

[62] Ozturk, T.; Talo, M.; Yildirim, E.A.; Baloglu, U.B.; Yildirim, O.; Acharya, U.R. Automated detection of COVID-19 cases using deep neural networks with X-ray images. Comput. Biol. Med. 2020, 121, 103792.

[63] Hu, M.; Lin, H.; Fan, Z.; Gao, W.; Yang, L.; Liu, C.; Song, Q. Learning to Recognize Chest-Xray Images Faster and More Efficiently Based on Multi-Kernel Depthwise Convolution. IEEE Access 2020, 8, 37265–37274.

[64] Ismael, A.M.; ¸Sengür, A. Deep learning approaches for COVID-19 detection based on chest X-ray images. Expert Syst. Appl. 2020, 164, 114054.

[65] Khan, A.I.; Shah, J.L.; Bhat, M.M. CoroNet: A deep neural network for detection and diagnosis of COVID-19 from chest x-ray images. Comput. Methods Programs Biomed. 2020, 196, 105581.

[66] Neha Pathak, MD, What Does COVID-19 Do to Your Lungs, WebMD Medical Reference, 2021, Available Online: https://www.webmd.com/lung/what-does-covid-do-to-your-lungs

[67] Tim Newman , What to know about X-rays,The medical News Today, 2018, Available online : https://www.medicalnewstoday.com/articles/219970.

[68] DSA, Health risks associated with X-ray diagnostics, 2021, Available Online : https://dsa.no/en/medical-use-of-radiation/health-risks-associated-with-x-ray-diagnostics.